

## Reviewed Preprint

v1 • July 1, 2026

Not revised

## ✉ For correspondence:

[girish@iiserpune.ac.in](mailto:girish@iiserpune.ac.in)[gdeshpande@iiserpune.ac.in](mailto:gdeshpande@iiserpune.ac.in)

## Competing interests: No

competing interests declared

Funding: See [page 27](#)

## Reviewing editor: Sofia J Araújo,

Universitat de Barcelona, Spain

© 2026, Roy et al. This article is distributed under the terms of the [Creative Commons Attribution License](#), which permits unrestricted use and redistribution provided that the original author and source are credited.

# Wunen(s) help navigate Primordial Germ Cells by attenuating Hedgehog signaling

Amrita Roy<sup>1</sup>, Adheena Elsa Roy<sup>1</sup>, Airat Ibragimov<sup>2</sup>, Juliana DaSilva<sup>2</sup>, Kundan Kumar<sup>1</sup>, Paul Schedl<sup>2</sup>, Siddhesh S Kamat<sup>1</sup>, Girish S Ratnaparkhi<sup>1</sup> ✉, Girish Deshpande<sup>1,2</sup> ✉

<sup>1</sup>Department of Biology, Indian Institute of Science Education & Research, Pune, India • <sup>2</sup>Department of Molecular Biology, Princeton University, Princeton, United States

## eLife Assessment

In this **valuable** manuscript, the authors tackle a highly relevant question in biology: how cells integrate attractive and repulsive cues to achieve directed migration. They present **solid** data demonstrating that two wunen genes act as negative regulators of Hedgehog signalling, thereby enabling efficient primordial germ cell (PGC) migration in *Drosophila* embryos. Beyond its immediate scope, this work has broader implications, particularly for understanding key mechanisms underlying complex processes such as cancer metastasis, where the coordinated interpretation of guidance cues is critical.

<https://doi.org/10.7554/eLife.111629.1.sa3>

## Abstract

Directed cell migration is a vital process that depends on the combined activities of attractive and repulsive cues. As it is essential for normal development, the precise identity of guidance signals and the underlying molecular and cellular mechanisms is being rigorously investigated. In a *Drosophila* embryo, PGC migration is orchestrated by non-cell autonomous repulsive and attractive cues, controlled by Wunen(s) - Wunen and Wunen2 and, HMGCoA-reductase (Hmgcr), respectively. Hedgehog (Hh), a PGC attractant, is potentiated by Hmgcr. We demonstrate that Wunen(s) employ both nonautonomous and autonomous modes to inhibit Hh signaling. Consistently, in embryos maternally compromised for *wunen*, mesodermal cells and PGCs accumulate excess Hh, leading to precocious clumping of the PGCs. This behaviour is reminiscent of PGC-specific loss of *patched* (*ptc*) – the Hh receptor and an antagonist of Smoothed (Smo), a G protein-coupled receptor (GPCR), involved in Hh signal transduction. Consistently, Wunen(s) inhibit membrane localization of Smo. Conversely, simultaneous overexpression of *wunen* mitigates PGC scattering induced by ectopic *hmgcr* expression. Finally, unbiased lipidomics of embryonic extracts after maternal knockdown of *wunen* confirms disruptions in lipid metabolism. We discuss the mechanistic underpinnings of Wunen(s) involvement in repressing Hh signalling to engineer PGC migration.

## Introduction

In diverse developmental contexts, directed cell migration constitutes a conserved and vital feature underlying the formation of a variety of cellular assemblies, including tissues and organs (Araujo 2015 [↗](#); Campanale and Montell 2023 [↗](#); Chen *et al.* 2025 [↗](#); Diaz *et al.* 2025 [↗](#); Roper 2025 [↗](#); Schick *et al.* 2025 [↗](#); Chowdhury *et al.* 2026 [↗](#)). Migrating cells navigate across multiple cell layers and travel long distances, which is controlled by soluble factors, chemokines, and intercellular communication, including cell adhesion (Paluch *et al.* 2016 [↗](#); Barton *et al.* 2024 [↗](#)). Intriguingly, at times, proper migration of a specific cell type is contingent upon secreted signaling ligands functioning either as attractive or repulsive cues. As these migratory events are essential

for generating fully functional and fertile multicellular organisms, a wide range of model systems, spanning from *Dictyostelium* to higher vertebrates, including mammals, are employed to elucidate underlying mechanisms (Santos and Lehmann 2004a [↗](#); Deshpande *et al.* 2025 [↗](#)). Given the biological relevance of these processes, severe cell migration aberrations have detrimental consequences, including sterility, metastasis and lethality (Paluch *et al.* 2016 [↗](#); Barton *et al.* 2024 [↗](#); Roper 2025 [↗](#); Chowdhury *et al.* 2026 [↗](#)).

Embryonic gonad coalescence in *Drosophila* has emerged as a formidable context to analyze the mechanistic underpinnings of cell migration (Kunwar *et al.* 2006 [↗](#); Chen *et al.* 2025 [↗](#); Deshpande *et al.* 2025 [↗](#)). Several features render it an ideal system for uncovering and elucidating multimodal mechanisms underlying cell migration. First, the embryonic *Drosophila* gonad consists of just two cell types: Primordial Germ Cells (PGCs) and Somatic gonadal precursor cells (SGPs), which are specified at distant locations, with the PGCs undergoing directed migration towards the SGPs. PGCs are initially formed at the posterior of the embryo and at the onset of gastrulation are located next to a layer of somatic cells. During gastrulation they are internalized by the invagination of the midgut. At the germband extension (stage 9), PGCs localized at the blind end of the gut begin to segregate away from one another and individualize in a coordinated manner before traversing through the gut epithelium. After emerging from the gut around stage 10, the migrating PGCs split into two bilateral clusters, enter the mesoderm and begin migrating towards the SGPs. The SGPs are specified in para-segments 10-13 and are arranged in two bilateral clusters. Once the PGCs and SGPs come into contact with each other, they intermingle and eventually compact into a tight cluster to form the paired primitive embryonic gonad.

The migration of the PGCs from the blind end of the gut and through the mesoderm is orchestrated by guidance signals emanating from the SGPs. The first hint of the possibility came from the discovery that 3-hydroxy-3-methylglutaryl-CoA reductase (*Hmgcr*) is responsible for the production or transmission of an attractive guidance cue. *hmgcr* is the rate-limiting step in several biosynthetic pathways including that of cholesterol and isoprenoids. Loss of *hmgcr* results in the scattering or mis-migration of PGCs in the posterior of the embryo, while ectopic expression of *hmgcr* induces PGCs to migrate abnormally towards the cells/tissues expressing *hmgcr*. In addition, *hmgcr* is initially expressed broadly in the mesoderm; however, as the embryo develops, its expression becomes progressively restricted, first to the posterior mesoderm and by stage 12, almost exclusively in the SGPs.

Though these studies demonstrated that *hmgcr* plays a key role in orchestrating PGCs migration, its immediate biosynthetic product (mevalonate) does not appear to be a plausible candidate as a guidance cue for the migrating PGCs (Santos and Lehmann 2004b [↗](#)). However, since mis-expression of *hmgcr* in many different cell types/tissues in the embryo induced PGCs to migrate towards the site of *hmgcr* expression, it was apparent that the actual attractant must be broadly expressed in the embryo but somehow limited in its ability to function as an attractant in the absence of *hmgcr*. The identification of Hedgehog (Hh) as the likely PGC attractant (Deshpande *et al.* 2001 [↗](#)) supported this notion. Like *hmgcr*, Hh is expressed in the SGPs and their progenitors. Likewise, misexpression of *hh* induces a subset of PGCs to migrate towards the ectopic source of Hh. Interestingly, the mis-migration of PGCs induced by *hh* ectopic expression is typically less severe than that induced by *hmgcr* expression in the same cell types/tissues (Deshpande *et al.* 2013 [↗](#)). This observation suggested that *hmgcr* was a limiting factor in the transmission of the Hh ligand. Several findings are consistent with this idea. First, in the ectoderm of *hmgcr* mutant embryos, the Hh ligand is retained in *hh*-expressing cells instead of being transmitted to the neighboring cells (Deshpande and Schedl 2005 [↗](#)). Second, co-ectopic expression of *hh* and *hmgcr* in the CNS leads not only to much more severe PGC mis-migration, but also substantially enhances the transmission of the Hh ligand from the ectoderm into the underlying mesoderm where it decorates the migrating PGCs (Deshpande *et al.* 2013 [↗](#)). Third, epistasis experiments show that *hh* functions downstream of *hmgcr* in PGC migration: the effects of ectopic *hmgcr* expression in the CNS on PGC migration can be suppressed by simultaneous knockdown of *hh* (Deshpande *et al.*

2023 [↗](#)). Fourth, two other genes, *toutvelu* and *dispatched*, known to be important for the cytoneme-based transmission of the Hh ligand are also epistatic to ectopically expressed *hmgcr* (Deshpande *et al.* 2023 [↗](#)).

The long-distance transmission of the Hh ligand requires the proteolytic cleavage of the precursor protein and a concurrent cholesterol modification. While several studies indicate that the cholesterol modification is important for the transmission of the Hh ligand from the SGPs to the migrating PGCs (Deshpande *et al.* 2016 [↗](#); Bialistoky *et al.* 2019 [↗](#)), flies lack the enzymes downstream of *hmgcr* for biosynthesis of cholesterol and thus this cannot be the function of *hmgcr* in the fly Hh signaling pathway. A solution to this puzzle came from the studies of (Santos and Lehmann 2004b [↗](#)) who showed that genes in the isoprenoid branch of the *hmgcr* biosynthetic pathway (Farnesyl diphosphate synthase: *fpps*; Geranyl-geranyl diphosphate synthase: *qme*) function downstream of *hmgcr* in PGC migration as does the isoprenoid transferase Geranyl-geranyl transferase (GGT1). The isoprenoid biosynthetic pathway is also required for the release/transmission of the Hh ligand, and at least one target in the Hh signaling pathway for geranylation by GGT1 is the *gy* subunit of the heterotrimeric G protein complex (Deshpande *et al.* 2009 [↗](#)).

Further evidence that the Hh signaling pathway orchestrates PGCs migration came from the experiments demonstrating that the reciprocal activities of the two receptors of the Hh ligand, namely Patched (Ptc) and Smoothened (Smo). Germline line clones and ectopic expression experiments show that the Hh receptor Patched (Ptc) is required in the PGCs for proper migration (Deshpande *et al.* 2001 [↗](#)). When *ptc* function is compromised in PGCs, they tend to clump together as would be expected if they constitutively “receive” a signal. Reception of the Hh ligand by the PGCs results in the internalization of Hh and Ptc into large intercellular puncta (Kim *et al.* 2021 [↗](#)) whereas the Smoothened (Smo) protein associates with the membrane in an actin-rich protrusion at the leading edge of the migrating PGCs (Kim *et al.* 2021 [↗](#)). Contrary to Ptc, when Smo activity is disrupted, the PGCs scatter in the mesoderm (Deshpande *et al.* 2001 [↗](#)). The non-canonical target for Smo activation is a G-protein coupled receptor, Trapped in Endoderm (Tre1). Like Smo, Tre1 localizes to the protrusions at the migration front together with dPIP5k, the enzyme responsible for generating PI(4, 5)P<sub>2</sub> (Kim *et al.* 2021 [↗](#)). The phosphatidylinositol 4-phosphate 5-kinase (PIP5K) targeted to the migration front by Tre1 induces the local accumulation of PI(4, 5)P<sub>2</sub> which, via WASP, activates Arp2/3 dependent actin polarization at the leading edge. In *tre1* mutants PIP5K does not localize to the migration front and as a result the production of PI(4, 5)P<sub>2</sub> does not become polarized. Likewise, actin is not preferentially polymerized at the migration front, thus linking the downstream events to the initial targeting of Smo to the membrane at the migration front in response to the reception of the Hh ligand (Kim *et al.* 2021 [↗](#)).

While Hh expressed by the SGPs induces PGC migration towards the SGPs by functioning as an attractant, there are two related lipid phosphate phosphatases (LPPs) *wunen* (*wun*) and *wunen-2* (*wun2*) that guide PGC migration by generating, in some as yet unknown manner, the repulsive signals (Starz-Gaiano *et al.* 2001 [↗](#); Hanyu-Nakamura *et al.* 2004 [↗](#); Renault and Lehmann 2006 [↗](#)). Both *wun* and *wun2* are maternally deposited and the maternal products are found in both the soma and the PGCs. They are also zygotically expressed in the epidermis, gut primordium, and nervous system. Intriguingly, *wun* or *wun2* specific transcripts are missing from the blind end of the gut primordium, a site which coincides with the region where the PGCs undergo transepithelial migration across the gut. Both ‘loss’ and ‘gain’ of function experiments have indicated that Wun(s) in the soma (of maternal and zygotic origin) function to repel migrating PGCs, and they avoid invading the ‘wrong’ tissues because of the presence of Wun(s). For instance, PGCs bypass the nervous system due to endogenous expression of *wun*(s) in the ventral nerve chord (Zhang *et al.* 1997 [↗](#); Hanyu-Nakamura *et al.* 2004 [↗](#); Renault *et al.* 2004 [↗](#); Renault *et al.* 2010 [↗](#); Leblanc and Lehmann 2017 [↗](#)). Conversely, when either *wun* or *wun2* is expressed in the mesoderm, PGCs are unable to enter the mesoderm. In addition to this non-autonomous repulsive function, the Wun(s) are also required in migrating PGCs where they contribute to their individualization i.e. PGC-PGC repulsion and help facilitate their proper migration (Renault *et al.* 2004 [↗](#); Renault *et al.* 2010 [↗](#)).

Though the *wun(s)* have been studied extensively since their discovery in the '90s (Zhang *et al.* 1997 [↗](#); Hanyu-Nakamura *et al.* 2004 [↗](#); Renault *et al.* 2004 [↗](#); Renault *et al.* 2010 [↗](#); Leblanc and Lehmann 2017 [↗](#)) the mechanistic basis for their repulsive activity in the soma and their cell autonomous function(s) in PGC has remained a mystery. One candidate target that could potentially connect both their non-autonomous function in the soma and their cell autonomous function in PGCs is the Hh signaling pathway. Here we show that the *wun(s)* function to suppress Hh signalling both in the soma and in migrating PGCs. In the soma, their activity counteracts *hmgcr*-dependent potentiation of Hh transmission. In PGCs, the *wun(s)* appear to function to suppress the response to the reception of the Hh ligand. In addition, we demonstrate that, Suppressor of actin 1 (Sac1), a lipid phosphatase, plays a similar role in PGC migration by downregulating Hh signalling. To better understand the activities of the two enzymes involved in lipid metabolism, *Wun(s)* and Sac1, we compared unbiased lipidomes from the respective embryonic extracts. Intriguingly, these lipid metabolism enzymes appear to exert their effects on the Hh signaling pathway by targeting different phospholipids (Burnett and Howard 2003 [↗](#); Burnett *et al.* 2004 [↗](#)).

## Results

### Embryos derived from mothers compromised for *wun* display enhanced levels of Hh targets

In stage 8-11 embryos, there is a positive autoregulatory loop in the embryonic ectoderm in which *hh* activates *wingless* (*wg*) expression in Hh-receiving cells, and *wg* in turn upregulates the expression of *engrailed* (*en*) in *hh*-expressing cells (Fig. 1A-B [↗](#)). We previously showed that mutations in *hmgcr* disrupt this autoregulatory loop, leading to significant downregulation of En expression. Thus, if the *Wun(s)* function to suppress the *hh* signaling pathway, we might expect to observe an opposite phenotype—namely that En protein expression will be upregulated when their activity is compromised.

As a test of this idea, *wun* was maternally (*M*-) depleted, by driving the expression of *UAS-wunRNAi* in the adult female germline using *nos-Gal4* (Fig. 1 [↗](#) Fig. 1C-E [↗](#)). We then examined En protein expression in the progeny (F2) of these females (mated to wild-type males). At stage 10, En expression in these *wun<sup>M-</sup>* embryos is appreciably increased compared to wild-type (Fig. 1 [↗](#), C1 versus D1, E1). In addition to a higher level of expression in individual cells, there is a readily discernable increase in the number of En-positive cells per stripe (Fig. 1 [↗](#), C1' vs D1', E1'). Upregulation of En expression together with a broadening of En stripe is also observed in *wun2<sup>M-</sup>* embryos (generated using the same strategy) although the phenotype is weaker compared to *wun<sup>M-</sup>* (Suppl. Fig. 1). Thus, compromising the activity of either *wun* or *wun2* maternally is sufficient to upregulate Hh signaling in the ectoderm.

In addition to being maternally deposited, the *wun(s)* are zygotically expressed in the gut endoderm and in a segmentally repeating pattern in the embryonic ectoderm. To determine whether zygotically expressed *wun* also functions to suppress Hh signaling, we mated females carrying a *maternal-atubulin Gal4* transgene (*Mat Gal4*) to *UAS-wunRNAi* males. Suppl. Fig. 2 [↗](#) shows that En expression is upregulated in these F1 embryos as compared to the control.

These findings indicate that both maternal and zygotic components of *wun* function to suppress *hh* signaling. If this is correct, then ectopic expression of *wun* in the zygote should suppress *hh* signaling and result in a decrease in En expression. To test this prediction, we mated females carrying *Mat Gal4* to males carrying a *UAS* transgene encoding a *wunen-GFP* fusion protein. As shown in Suppl. Fig. 2C [↗](#), zygotic overexpression of *wun* (*Wun<sup>OE</sup>*) in the embryo results in a decrease in En protein expression.

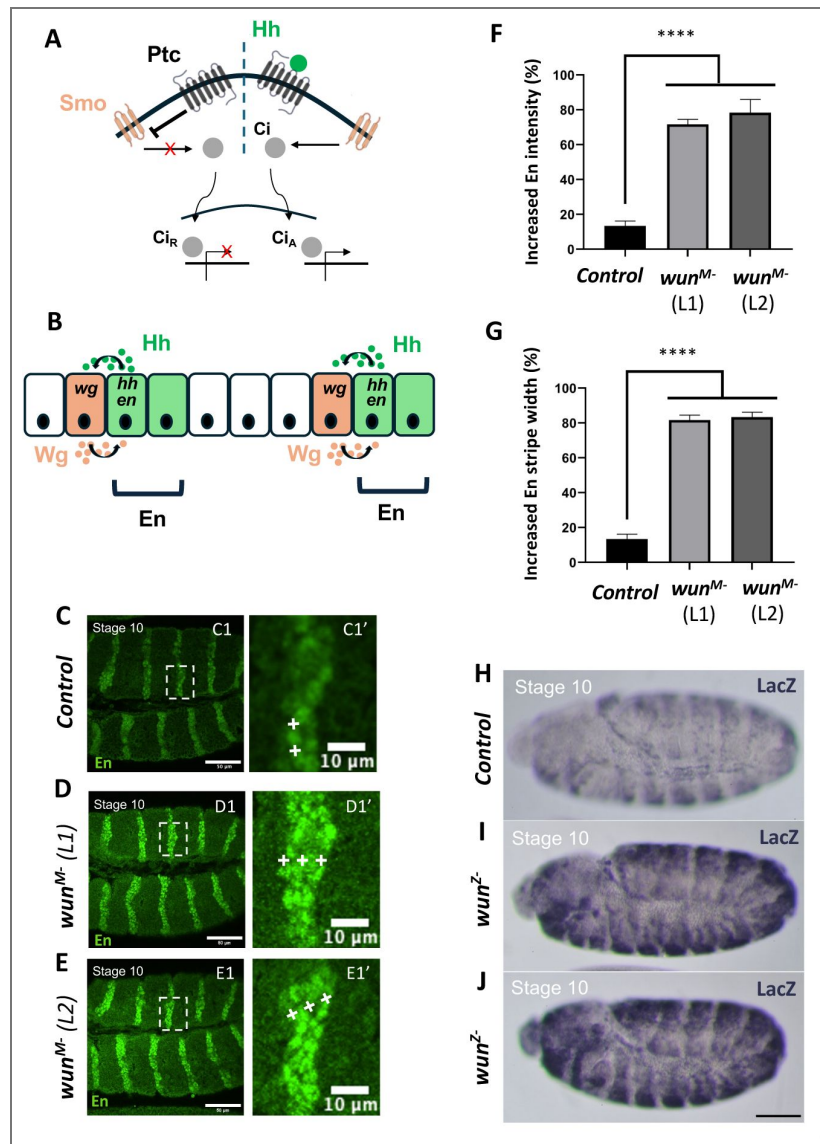


**Figure 1. Embryos either maternally (*M*) or zygotically (*Z*) compromised for *wun* display enhanced levels of ectodermal *En* and *Ptc*.**

(A-B) Schematics depict the canonical Hh signalling pathway (A), where in the ‘signaling Off/Hh-unbound’ state, Ptc inhibits Smo, and in the absence of signal transduction downstream of Smo, Ci retains its repressor activity (Ci<sub>R</sub>). In the ‘On’ state, Hh is bound to its receptor Ptc, which in turn relieves Smo inhibition. Smo dependent signaling results in generation of transcriptional activator (Ci<sub>A</sub>) form. Panel (B) represents Hh’s role in the formation of segmental boundaries in the embryonic epidermis. En, expressed in the posterior of each para-segment, activates *hh*. Hh is secreted from the En-positive cells, and binds to Ptc receptor in the neighboring cells, wherein activation of Hh signaling leads to *wg* expression. Wg, in turn, is secreted from these neighboring cells, and signals reciprocally to the En-positive cells, setting up a tri-partite positive feedback loop between En/Wg/Hh. Together the activities of these three gene products determine the para-segmental boundary and thus defining the segment polarity. (C-E) *nos-gal4* virgin females were mated with males of specified genotypes, including negative control (*UAS-lex RNAi*) and two different *UAS-wun RNAi* lines, denoted as *wun Line1(L1)* and *wun Line2 (L2)*. Stage 10 embryos derived from mated females carrying both transgenes (*nos-gal4/UAS-RNAi*) were stained with anti-Engrailed (En) antibody. Compared to the Control *lex<sup>M-</sup>* embryos (A), a significantly higher percentage of *wun<sup>M-</sup>* embryos (B and C) display an increased level of En protein as well as broader En stripes. The two *UAS-wun RNAi* lines behaved similarly. Panel A1’-C1’ shows magnified insets that demonstrate both the elevation in the En levels and broadening of the stripes, indicating additional number of nuclei that stain for En. The ‘+’ mark denotes En positive cells. (F-G) Quantification of percentage of embryos showing increased En intensity and broader stripes (n=15, N=3, \*\*\*\*p<0.0001). Significance was estimated using Ordinary one-way ANOVA (H-J) Recombinant *ptc-gal4 UAS-β-gal* females were mated with the *UAS-RNAi* males of the indicated genotype. Stage 10/11 embryos (F1) derived from the respective crosses were stained with anti-β-gal antibody. Compared to the control, *ptc-gal4 UAS-β-gal* (H), all embryos *ptc-gal4 UAS-β-gal/UAS-RNAi* (n~30) show considerably enhanced β-gal expression, which indicates Ptc activation (I and J).

## Embryos zygotically compromised for *wun* display increased levels of $\beta$ -galactosidase driven by patched-Gal4

The interaction between Hh and Ptc results in the translocation of the Smo protein to the membrane and signal transduction (Hu and Song 2019 [↗](#); Ingham 2022 [↗](#); Zhang and Beachy 2023 [↗](#)) (Fig. 1A, B [↗](#)). In the canonical pathway, this results in the transcriptional upregulation of *ptc* via Cubitus interruptus (Ci). Ptc upregulation provides a negative feedback loop that limits Hh activity and spread. (Chen and Struhl 1998 [↗](#); Briscoe *et al.* 2001 [↗](#); Casali and Struhl 2004 [↗](#)) If *wun* functions to suppress this branch of the canonical *hh* pathway, compromising *wun* activity zygotically (Z-) should result in a detectable increase in *ptc* expression. We mated females carrying a *ptc-gal4 UAS- $\beta$ -gal* (Johnson *et al.* 2000 [↗](#)) recombinant to either control males or males carrying the *UAS-wun RNAi* transgene and stained the resulting (F1) embryos with anti- $\beta$ -galactosidase (anti- $\beta$ -gal) antibodies. The control embryos displayed a segmental pattern that mimics *ptc* expression (Fig. 1H [↗](#)). By contrast, the *ptc-gal4 UAS- $\beta$ -gal/UAS-wun RNAi* embryos (Fig. 1I-J [↗](#)) displayed a considerable increase in the anti- $\beta$ -gal specific signal in nearly all the embryos.

## Simultaneous overexpression of *wun* in the nervous system can mitigate PGC migration defects induced by *elav-gal4 UAS-hmgcr*

While the experiments involving RNAi-based embryonic knockdown suggested that *wun(s)* function to down regulate the *hh* signaling pathway in embryos, they do not provide insights into the underlying mechanism. Interestingly, similar to *wun(s)*, another phospholipid phosphatase, *sac1*, functions to attenuate the *hh* signaling pathway (Yavari *et al.* 2010 [↗](#)). Studies in wing and eye discs have argued that *sac1* downregulates the *hh* pathway, in the receiving cells, after reception of the Hh ligand. While a similar cell-autonomous mechanism downstream of reception could be deployed by the *wun(s)*, their ability to inhibit PGC migration into endodermal and ectodermal tissues suggests that they could also suppress the transmission of the Hh ligand. (The cell-autonomous and non-cell autonomous functions of Wun(s) need not be mutually exclusive). If this model is correct, then *wun(s)* would counteract the potentiation of Hh transmission by *hmgcr*. Expression of *UAS-hmgcr* in the embryonic CNS using an *elav-Gal4* driver induces PGC migration defects. These PGC migration defects can be substantially enhanced by co-expressing *UAS-hh* in the CNS while they are suppressed by co-expressing *UAS-hhRNAi* (Deshpande *et al.* 2023 [↗](#)). Likewise, RNAi knockdown in the CNS of two genes required for Hh transmission, *ttv* and *disp* also suppressed the PGC migration defects induced by ectopic *hmgcr* (Deshpande *et al.* 2023 [↗](#)). To explore the idea that *wun* functions to attenuate the transmission of the Hh ligand, we examined if overexpression of *wun* (*UAS-wun*) is also able to mitigate the PGC migration defects induced by ectopic expression of *hmgcr* in the embryonic nervous system using the *elav-Gal4* driver (embryos derived from the *elavGal4UAS-hmgcr* recombinant strain).

Stage 13-14 embryos were classified based on the number of mis-migrated/scattered PGCs: 0-4, 5-9, 10-14 and 15+ mis-migrated PGCs. Compared to control embryos (Fig. 2A [↗](#) and 2D [↗](#)), about 65% of *elav-gal4 UAS-hmgcr/+* embryo had 10 or more PGCs scattered/mis-migrated (Fig. 2B [↗](#) and 2E [↗](#)). As observed for *hh*, *ttv* and *disp* RNAi knockdowns, co-expression of Wun suppresses the PGC migration defects induced by *hmgcr*. Only about 20% of *elav-gal4 UAS-hmgcr/UAS-wunGFP* embryos had 10 or more mis-migrated PGCs (Fig. 2C [↗](#) and 2F [↗](#)). The suppression of mis-migration induced by *elav-gal4UAS-hmgcr* by simultaneous overexpression of *wun* is quantified in Fig. 2G [↗](#).

## *wun*<sup>M</sup>- embryos display elevated levels of endogenous Hh-GFP in the PGCs and surrounding mesodermal cells

When *hmgcr* is co-expressed with *hh-GFP* in the embryonic CNS using an *elav-Gal4* driver, it substantially enhances the transmission of the Hh-GFP ligand encoded by the transgene into and through the underlying mesoderm, where it decorates the migrating PGCs (Deshpande *et al.* 2013 [↗](#)). Thus, a clear implication of the *hmgcr-wun* epistasis experiments in the previous section

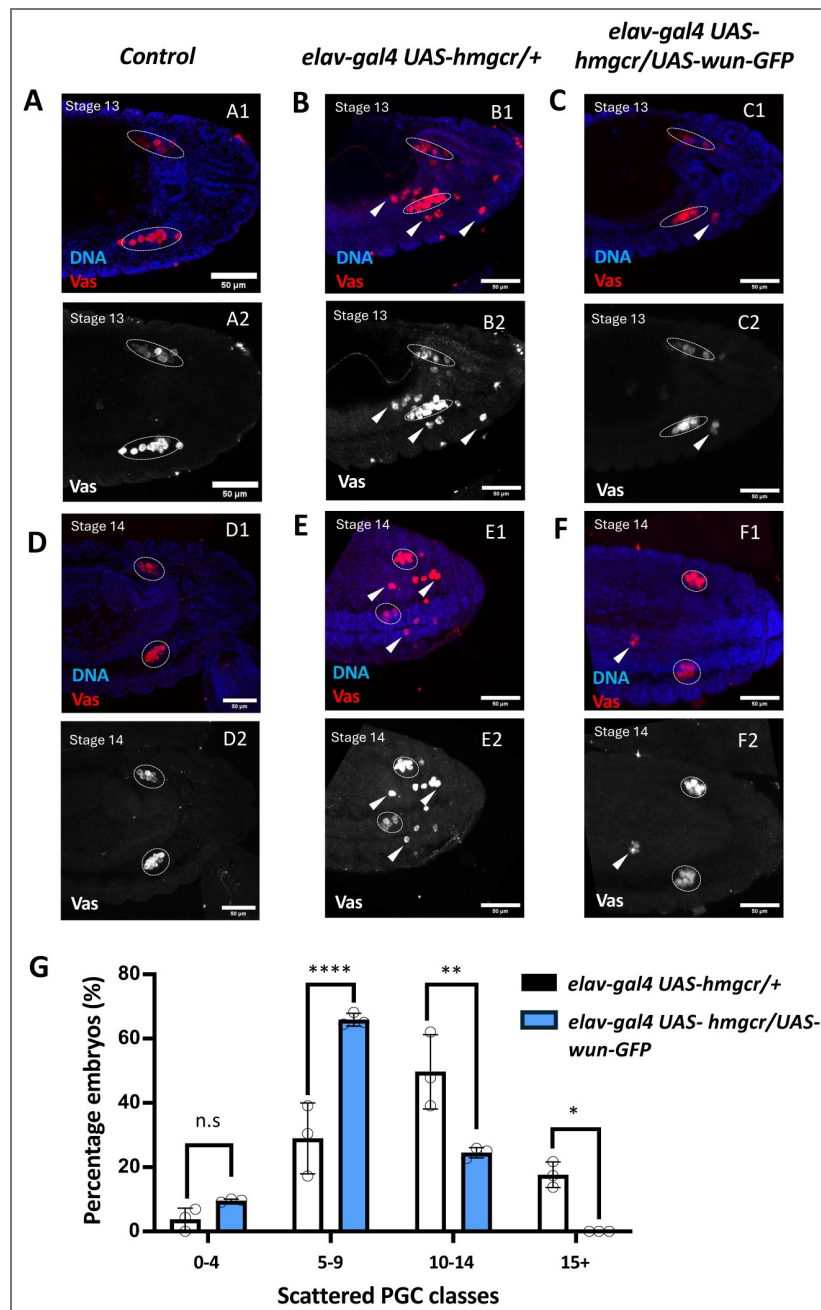


**Figure 2. Aberrant PGC migration, induced by ectopic expression of *hmgcr* can be effectively suppressed by simultaneously overexpressing *wun*.**

(A-C) Stage 13 embryos. Compared to control CS (A) PGCs in *elav-gal4 UAS-hmgcr/+* are greatly scattered away from the gonad (B). In *elav-gal4 UAS-hmgcr/UAS-wun-GFP* embryos, simultaneous overexpression of *wun-GFP* suppresses the migration defects induced by the ectopic expression of *hmgcr* in the nervous system (C) A2, B2, C2 are greyscale representations of the Vasa channel. (D-F) Stage 14 embryos of the indicated genotypes. Migration defects caused by ectopic expression of *hmgcr* in the nervous system are suppressed by simultaneous expression of *wun-GFP*. (A1-D1) Merged image with anti-Vas and counterstained with Hoechst. (A2-D2) PGCs stained with anti-Vas. D2, E2, F2 are greyscale representations of the vasa channel (G) Quantification of *elav-gal4 UAS-hmgcr/+* and *elav-gal4 UAS-hmgcr/UAS-wun-GFP* embryos belonging to the mentioned classes of scattered PGCs (n=25, 3 replicates). Significance calculated using Two-way ANOVA and Tukey's multiple comparison test \*\*\*\*p<0.0001, \*\*p<0.01, \*p<0.05.

is that the *wun(s)* are able to negatively regulate the *hh* signaling pathway because they block the efficient transmission of the Hh ligand. If this inference is correct, the transmission of endogenously expressed Hh should be substantially increased when *wun(s)* activity is compromised. To test this idea, we used the *nos-Gal 4/UAS-wun RNAi* combination to deplete maternal deposition of *wun*. Females carrying this transgene combination were then mated to males carrying a BAC *hh-GFP* rescue construct (henceforth referred to as Hh-GFP) which recapitulates the pattern of expression of the endogenous *hh* gene (Chen *et al.* 2017 [↗](#)). As shown in Fig. 3A-B [↗](#), there is substantial increase in the transmission of the Hh ligand in *wun<sup>M-</sup>* embryos, as suggested by increased Hh accumulation in the somatic mesoderm. As previously reported by (Kim *et al.* 2021 [↗](#)) for wild type *hh-GFP* embryos, a substantial fraction of embryonic PGCs, display detectable levels of Hh-GFP from stage 9/10 onwards (Fig. 3D [↗](#)). Moreover, as predicted, there appeared to be a significant elevation in the number of Hh-GFP-puncta per PGC in the *wun<sup>M-</sup>* embryos (Fig. 3E [↗](#)-3F [↗](#)). To better analyze the change, we quantitated the total number of readily discernible Hh-GFP puncta per PGC in the control (*UAS-lexA RNAi*) and *wun<sup>M-</sup>* embryos. In control embryos, about 90% of the Hh-GFP signal-positive PGCs have 5 or less puncta and of these about 50% have only 1 or 2 Hh-GFP puncta. Since PGCs do not express Hh, the increase in Hh-GFP puncta/PGC in *wun<sup>M-</sup>* embryos must, at least in part, be due to the upregulation of Hh-GFP transmission from the surrounding mesodermal and ectodermal tissues. To confirm this idea, we measured the frequency of Hh-GFP puncta in a region (ROI) dorsal to the gut that is devoid of PGCs. As shown in Fig. 3C [↗](#), the number of Hh-GFP puncta in this region of the mesoderm is greatly enhanced in *wun<sup>M-</sup>* embryos. Taken together with the results in the previous sections, these findings indicate that *wun(s)* function to downregulate or block the transmission of Hh from cells that synthesize the ligand.

Since the *wun(s)* are also required in PGCs (Renault *et al.* 2004 [↗](#); Renault *et al.* 2010 [↗](#)), we cannot exclude a complementary cell autonomous effect in which the loss of maternally derived *wun* in migrating PGCs also contributes to the increase in PGC associated Hh-GFP puncta.

## Aberrant localization of Smo in PGCs of *wun<sup>M-</sup>* embryos

The reception of the Hh ligand results in the translocation of Smo from its cytoplasmic localization to the cell membrane. In PGCs Smo localizes to membrane protrusions at the leading edge of the migrating cells (Kim *et al.* 2021 [↗](#)) and mediates the recruitment of the Tre1 GPCR receptor. Tre1 induces localized actin polymerization in response to a transduction pathway the produce PI(4,5)P2. Since Hh signaling to the migrating PGCs is polarized, there is typically only a single sharp focus of Smo protein which is localized at the leading edge (Fig. 4 [↗](#), A1-A4). Typically, wild-type PGCs display a single sharp focus with the residual protein being associated with the rest of the membrane. This pattern of localization is disrupted in *wun<sup>M-</sup>* (Fig. 4 [↗](#), B1-B4; C1-C4). To better understand the aberrant behavior, we classified individual PGCs based on the pattern of Smo localization. The classes included (i) PGCs showing no Smo-specific signal, (ii) PGCs showing a single focused crescent of Smo at the leading edge (iii) PGCs displaying diffuse localization of Smo across the membrane (iv) PGCs having a combination of a leading edge and a diffuse localisation of Smo (v) PGCs with multiple foci enriched for Smo-specific staining. In control PGCs, most PGCs have a single focus or a single focus surrounded by a more diffuse pattern of localization (~60%). In contrast, less than 40% of the PGCs in *wun<sup>M-</sup>* embryos have a single focus or a single focus surrounded by a more pattern of localization. About 35% show strong staining across the entire cell, while over 10% have multiple Smo foci. The changes in Smo localization are quantitatively significant (Fig. 4D [↗](#)).

## PGC migration defects in *wun<sup>M-</sup>* embryos mimic those in *ptc<sup>M-Z+</sup>* embryo

In earlier studies we found that PGCs in stage 11 embryos generated by mating *ptc<sup>-</sup>* germline clone females to wild type males tended to get stuck in the gut and/or clump together (Deshpande *et al.* 2001 [↗](#)). Since loss of *ptc* would result in the constitutive activation of the *hh* signaling pathway,

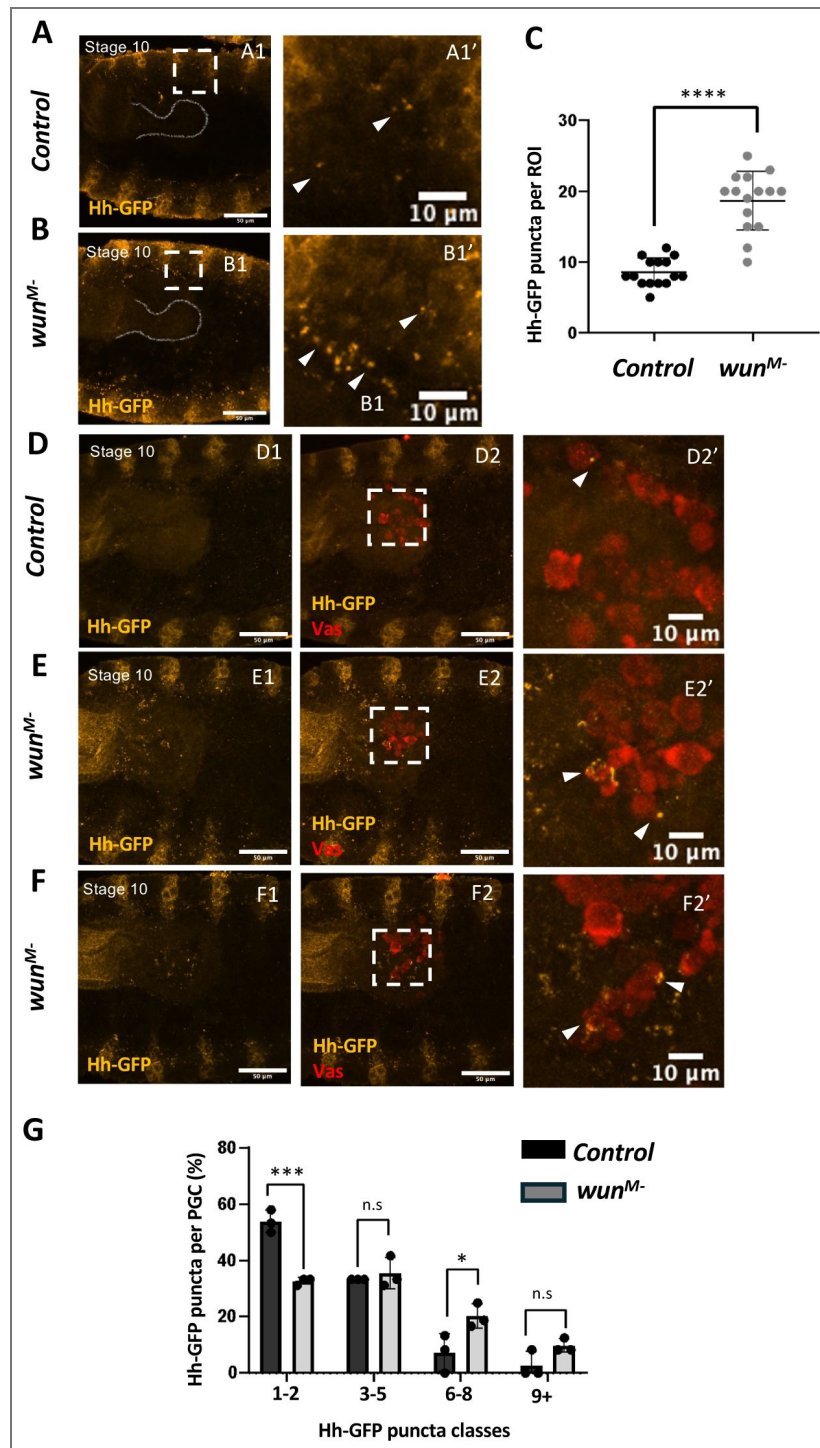


**Figure 3.** *wun<sup>M-</sup>* embryos exhibit an increase in endogenous Hh-GFP puncta in the mesoderm and the adjacent PGCs.

(A-B) Either *UAS-lexA RNAi* or *UAS-wun RNAi* males were mated with *nos-gal4* virgin females carrying both the transgenes were mated with endogenous *Hh-GFP* males. Compared to control *lexA<sup>M-</sup>* (A), *wun<sup>M-</sup>* embryos show a higher number of *Hh-GFP* puncta (Yellow) in the mesoderm. (C) Individual *Hh-GFP* puncta were counted in 15 ROIs dorsal to the gut, per genotype (gut outline is marked in all the panels). The increase in *Hh-GFP* is quantified using an unpaired T-test, \*\*\*\**p*<0.0001. (A1-B1). Magnified insets shown in (A1'-B1'), with arrowheads marking *Hh-GFP* puncta. (D-F) Compared to control, *lexA<sup>M-</sup>* (D) *wun<sup>M-</sup>* embryos show a higher number of *Hh-GFP* puncta in their PGCs (E and F), marked with anti-Vasa antibody (red) staining. Magnified insets (D2'-F2'), with arrowheads marking *Hh-GFP* puncta. (G) The total number of puncta was counted in 15 PGCs per genotype across three replicates, and the percentages of PGCs with 1-2, 3-5, 6-8 and 9+ *Hh-GFP* puncta are plotted. Significance was calculated using Two-way ANOVA and Tukey's multiple comparison test (\*\*\*\**p*<0.0001, \*\*\**p*<0.001, \*\**p*<0.01).

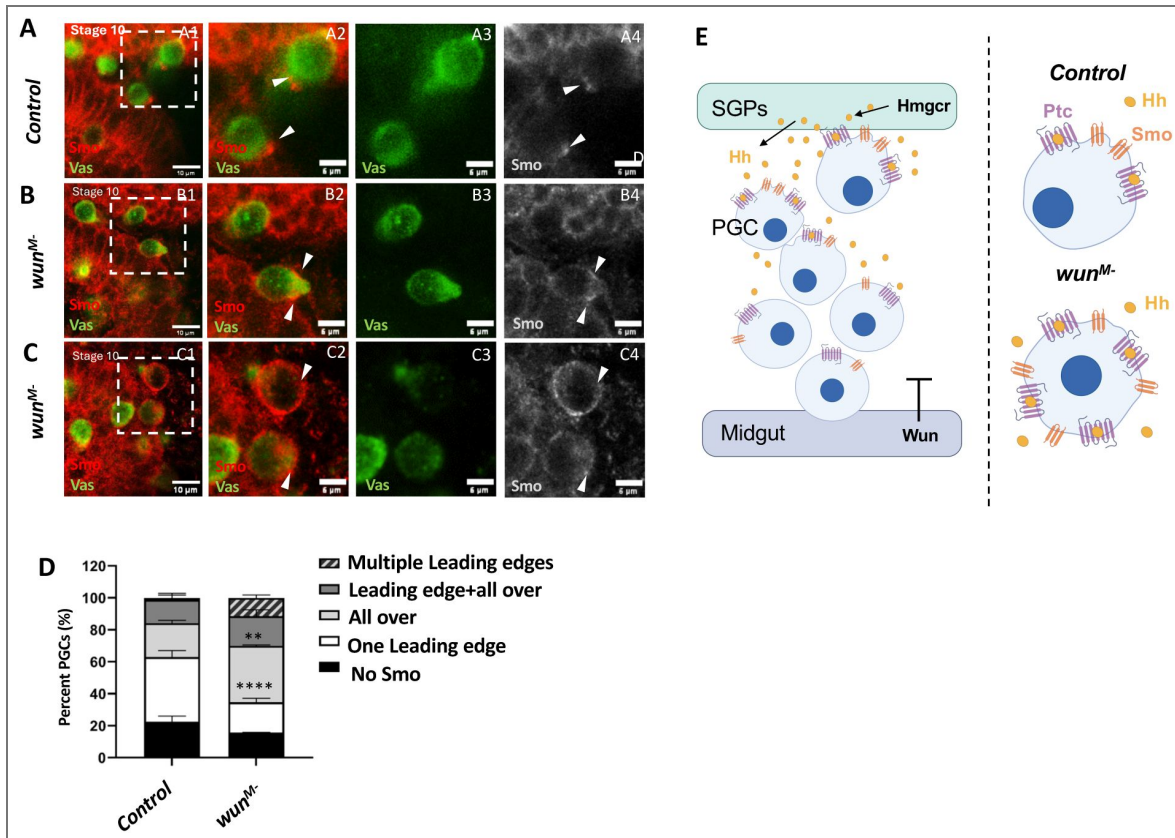


**Figure 4. Embryos compromised for *wun* display aberrant *Smo* localization.**

(A-E) PGC migration through the gut in stage 10 embryos of the indicated genotype. In control *lexA<sup>M-</sup>* embryos (A) *Smo* is localized at the leading edge (A1, magnified inset A2-A4). In contrast, in *wun<sup>M-</sup>* PGCs, multiple foci of *Smo* localisation are observed (B1, magnified inset B2-B4) or are present all over the PGC (C1, magnified inset C2-C4). All panels were equally edited with minimum intensity value at 10 and maximum intensity value at 100 using Fiji Image J. (D) Comparison of percentages of embryos of indicated genotypes having *Smo* localization as per mentioned classes were quantified (n=40-70 across replicates) using 2-way ANOVA and Tukey's multiple comparison test \*\*\* p<0.001 \*\* p<0.01. (E) Germ cell repulsion mediated by Wunen(s) is mediated by their ability to inhibit Hh signaling in the somatic tissues such as gut, ectoderm, nervous system. This influences the path of the migrating PGCs and guides them towards their destination i.e. SGPs, enriched in *Hmgcr*, which potentiates Hh activity. Additionally, germ cell-germ cell repulsion is also mediated by Wun and germ cell autonomous ability of Wun(s) to inhibit Hh signaling may be critical in this regard and upon compromising *wun* activity response to Hh signaling gets activated precociously.

one might imagine that the excessive multi-directional *hh* signaling evident in *wun<sup>M-</sup>* embryos could result in the PGC phenotypes observed in the absence of *ptc*. To test this idea directly, we maternally depleted *ptc* and the *wun(s)* using the same RNAi strategy described above (*nos-Gal4/UAS-ptcRNAi*, *nos-Gal4/UAS-wunRNAi* and *nos-Gal4/UAS-wun2RNAi* females mated to wild type males) Suppl. Fig. 3 [↗](#) and Fig. 5 [↗](#). As controls, we generated embryos from mothers expressing *lexARNAi* (*nos-gal4/UAS-lexARNAi*).

As shown in Suppl. Fig. 3 [↗](#) we find that individualization of the PGCs in nearly half of the *ptc<sup>M-</sup>* embryos (45%) is hindered, resulting in an inefficient exit across the midgut primordium. Consequently, PGCs lag behind in the gut forming small clumps. In a small but significant proportion of the *ptc<sup>M-</sup>* embryos PGCs form a large clump inside the gut (Suppl. Fig. 3B [↗](#)). Similar phenotypes are observed in stage 10-13 embryos derived from *nosGal4/UAS-wun RNAi* females. In >55% of *wun<sup>M-</sup>* embryos the individualization of PGCs was hindered, resulting in a delay in exiting the gut (Fig. 5C-G [↗](#)). In about 15% of embryos, the PGCs clump together within the midgut (Fig. 5B, G [↗](#)). Maternal depletion of *wun2* results in similar PGCs phenotypes to those observed in *wun<sup>M-</sup>* embryos; however, they are substantially more penetrant. Over 60% *wun2<sup>M-</sup>* embryos have large clumps of PGCs either within the gut or along the dorsal surface of the gut (Fig. 5F, H [↗](#)). In another ~15% of the *wun2<sup>M-</sup>* embryos, several PGCs are delayed in exiting the gut.

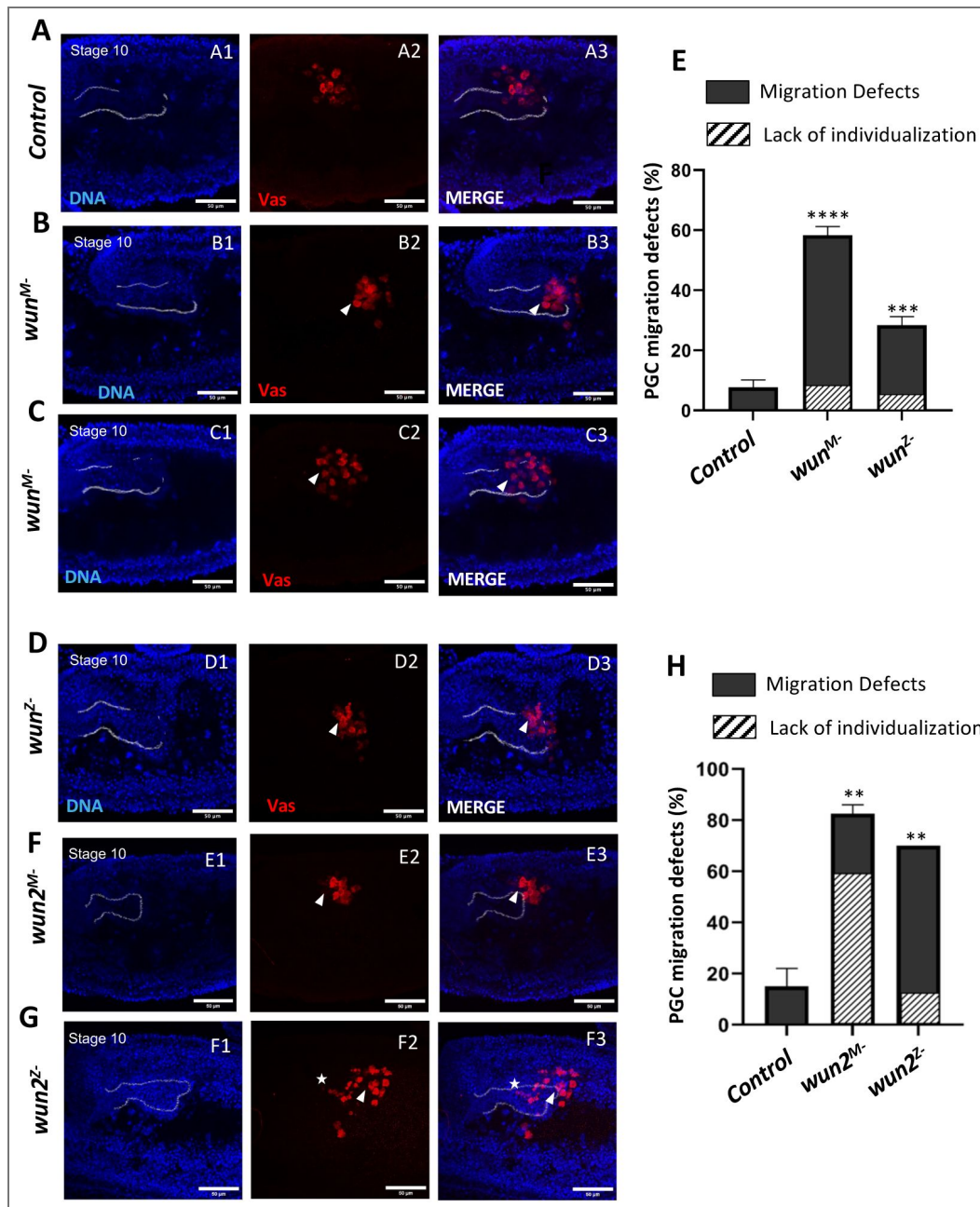
## wun or wun2 are required in PGCs during the initial phase of migration

The results in the previous section indicate that the *wun(s)* play a key role in directing PGC migration at a very early step when the cells first begin to exit the midgut. Since the maternal RNAi knockdowns results in a substantial upregulation in the transmission of the Hh ligand throughout the embryonic soma, this early PGC defect could simply be a consequence of excessive somatic *hh* signaling. On the other hand, maternal knockdown of the *wun(s)* will also reduce the activity of the *wuns* in the PGCs themselves. In this case, the early phenotypes could also reflect a PGC-autonomous requirement of the *wun(s)*. To test this possibility, we used *nos-Gal4* to drive *UAS-wunRNAi* (Fig. 5D [↗](#)) or *UAS-wun2RNAi* (Fig. 5G [↗](#)) in migrating PGCs and stained F1 embryos with anti-Vasa. In both cases we observe phenotypes similar to those in the maternal knockdowns, though they are not as severe. For the *wun* knockdown, PGC clumping was observed in about 5% of the embryos, while lagging PGCs were observed in about 20% of the embryos (Fig. 5E [↗](#)). The knockdown of *wun2* was more effective: Premature clustering of the PGCs was observed in nearly 10% of the embryos, while 50% of the embryos had lagging PGCs (Fig. 5H [↗](#)). These findings confirm the idea that the *wun(s)* are required in PGCs for proper migration and suggest that this function is likely related to the proper functioning of the *hh* signaling pathway.

## Sac1, a known lipid phosphatase, downregulates Hh signaling in the embryonic contexts including in the PGCs

As mentioned above, the *wun(s)* are not the only phospholipid phosphatase that function to downregulate *hh* signaling. The lipid phosphatase, Sac1, was found to negatively regulate the *hh* pathway in wing and eye discs (Yavari *et al.* 2010 [↗](#); Del BEL *et al.* 2018 [↗](#)). As Sac1 is also expressed in the embryonic gut primordium and the ectoderm we decided to test if maternal loss of *sac1* results in embryonic phenotypes similar to those observed for the *wuns*. We first examined the expression En in the ectoderm. Suppl. Fig. 4 [↗](#) shows that as in the case of knockdown of the *wun(s)*, both the width of the En stripes and the nuclear signal intensity are enhanced in *sac1<sup>M-</sup>* embryos.

Next, we tested whether the PGCs from *sac1<sup>M-</sup>* embryos display PGC migration defects. We find that the PGCs in *sac1<sup>M-</sup>* embryos also exhibit migration phenotypes, though they are less severe than those in *wun<sup>M-</sup>* or *wun2<sup>M-</sup>*. PGCs lagging in the midgut are observed in stage 10 *sac1<sup>M-</sup>* embryos, and small clumps of PGCs are seen in the midgut of some stage 11 *sac1<sup>M-</sup>* embryos (Fig. 6 [↗](#); compare A, B with D, E respectively). In stage 13 embryos, there are scattered PGCs, and the number of PGCs coalescing into the embryonic gonad is reduced (Fig. 6C [↗](#) versus 6F). The same



phenotypes are observed when *nos-Gal4* is used to drive paternally derived *UAS-sac1RNAi* in the migrating PGCs (Fig. 6 [↗](#); G, H vs I, J respectively). Interestingly zygotic knock down of reciprocally active Kinase, *stt4*, also leads to PGC migration defects (Yavari *et al.* 2010 [↗](#)) (Fig. 6 [↗](#) K-M; See Suppl. Fig. 5 [↗](#) for quantitation). Furthermore, supporting a genetic interaction between *wun* and *sac1*, a higher proportion of embryos displayed precocious clustering of PGCs (Fig. 6 [↗](#) P) and Smo mislocalization at germ band extension stage (Suppl. Fig. 6 [↗](#)).

## Endogenous Hh-GFP specific puncta in the mesoderm and the adjacent PGCs are enhanced in *sac1<sup>M-</sup>* embryos

The analysis of *sac1* function in the eye and wing discs suggested that it functions in receiving cells to inhibit the membrane association of Smo. When *sac1* activity was compromised in receiving cells, Smo association with the membrane was substantially enhanced. Moreover, in this developmental context the phenotypes induced by the loss of *sac1* activity were found to be independent of the Hh ligand. Consistent with a similar cell autonomous role, we found that knockdown *sac1* activity in PGCs induced migration defects. However, since we also observed PGC migration phenotypes when *sac1* activity is maternally depleted, it seemed possible that *sac1* might also have a cell non-autonomous function in the *hh* signaling pathway analogous to *wun(s)*. To explore this possibility, we mated *Mat Gal4/UAS-sac1-RNAi* females with *hh-GFP* males. The experiments in Fig. 7 [↗](#) show that somatic loss of *sac1* results in a substantial upregulation in the transmission of the Hh ligand. In panels A-C (Fig. 7 [↗](#)) we examined the accumulation of Hh-GFP puncta in the mesoderm. As indicated by the quantitation in panel C, the number of Hh-puncta is increased ~2.5 fold. Accompanying this increase in mesodermal Hh-GFP puncta, we find that there is a significant increase in the number of Hh-GFP puncta per PGC in *sac1<sup>M-</sup>*. (Fig. 7F [↗](#)). About 55% control PGCs had 1-3 Hh-GFP puncta as opposed to ~20% of the *sac1<sup>M-</sup>* PGCs. ~80% of *sac1<sup>M-</sup>* PGC had 4 or more Hh-GFP puncta compared to about 53% in control. More importantly, none of the PGCs in control embryos had 10+ Hh-GFP puncta. Altogether, our data shows that maternally compromising *sac1* activity results in excess accumulation of Hh-GFP in the mesoderm and PGCs.

## Comparative unbiased lipidomics of *wun<sup>M-</sup>* and *sac1<sup>M-</sup>* embryonic extracts

While depletion of the *wun(s)* and *sac1* give a similar range of *hh* signaling pathway phenotypes, the substrates for these enzymes involved in lipid metabolism are likely different. The preferred substrate for *sac1* is phosphatidylinositol 4-phosphate (PI4P) which it dephosphorylates to phosphatidylinositol (PI) (Yavari *et al.* 2010 [↗](#)).

While the *wun(s)* share homology with a mammalian family of lipid phosphate phosphatases (LPP1, LPP2 and LPP3), biochemical experiments suggest that their substrate preferences are likely different. The mammalian LPP family proteins dephosphorylate a broad range of phospholipids, including among others lysophosphatidic acid (LPA), phosphatidic acid (PA) and ceramide-1-phosphate C(1)P (Dillon *et al.* 1997 [↗](#); Jasinska *et al.* 1999 [↗](#)). Unlike the mammalian LPP family members, (Burnett and Howard 2003 [↗](#)) found that *wun* is unable to dephosphorylate either PA or C(1)P. However, *wun* was able to dephosphorylate LPA with a similar efficiency to that of the mammalian LPP1 and LPP3 enzymes. To identify possible targets for the *wun* and *sac1* we performed unbiased lipidomics on embryonic extracts derived from *wun<sup>M-</sup>* and *sac1<sup>M-</sup>* 4-8 hr embryos (for details, see Materials and Methods).

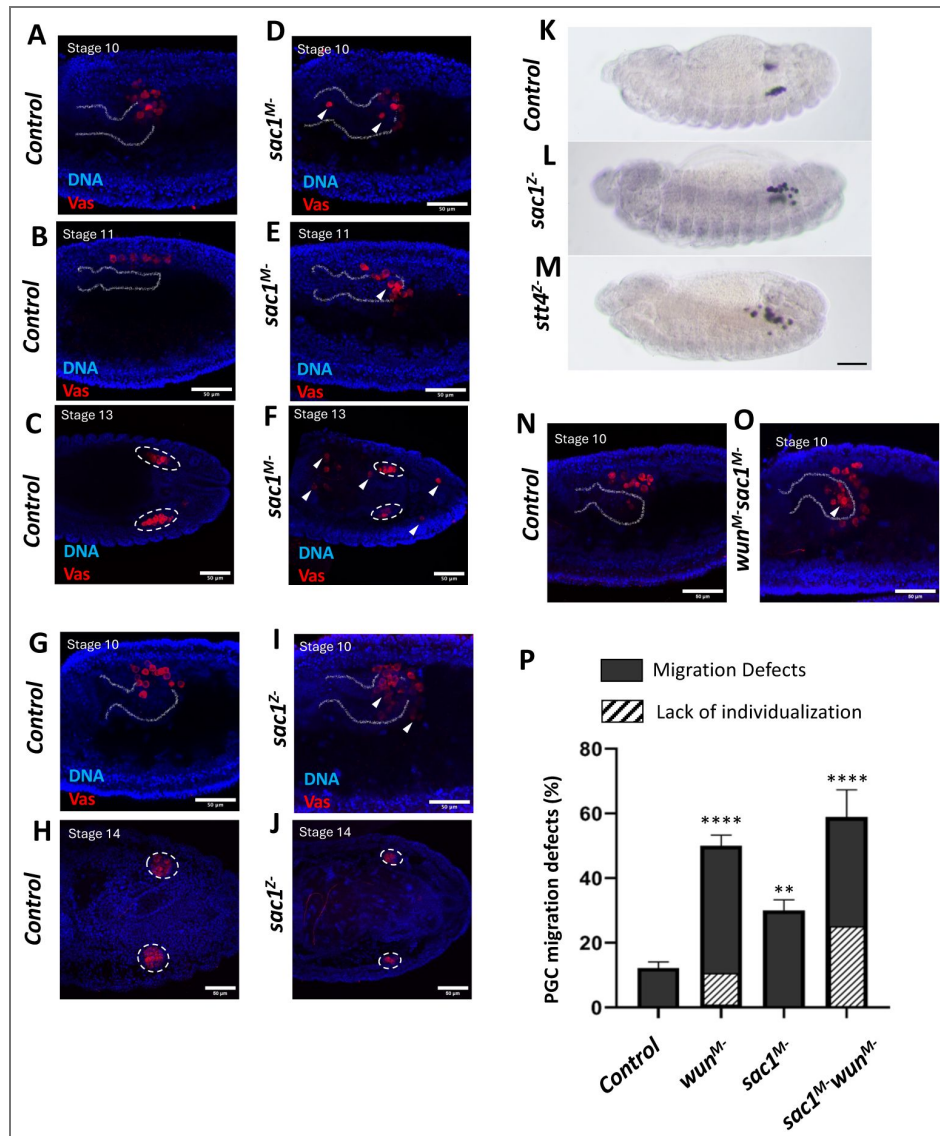


**Figure 6. Sac1 influences PGC migration.**

**(A-J)** Embryos of indicated stages and specified genotypes stained with anti-Vas and Hoechst to mark DNA. (A-F) Embryos that are maternally deprived of indicated genes. Compared to control (A-C) *lexA<sup>M</sup>*, the PGCs of *sac1<sup>M</sup>* embryos have a variety of migration defects such as delay in exiting the gut (D), clumping (E) and inability to migrate towards the SGPs (F). **(G-J)** Embryos derived from *nos-gal4* mothers crossed to *UAS-RNAi* of indicated genes. Compared to control (G-H), PGCs from *sac1<sup>Z</sup>* embryos also show migration defects including delay in exiting the midgut (I) and have reduced number of PGCs in the coalesced embryonic gonads as compared to control (J). Arrowheads mark mis-migrated PGCs. In the relevant panels outline of the gut (stage 10) or the embryonic gonad (stage 14) are marked with dotted lines and circles respectively. **(K-M)** Stage 13 embryos derived from *nos-gal4-VP16* females crossed to *UAS-RNAi* males of indicated genotypes resulting in embryos that are zygotically depleted for the individual gene expression in a PGC specific manner. *sac1* and *stt4* regulate Hh signaling in a qualitatively opposite manner. Compared to the control *egfp<sup>Z</sup>* embryo (K), PGCs in *sac1<sup>Z</sup>* embryos (L) are slow to reach the embryonic gonad. While PGC in *stt4<sup>Z</sup>* embryos scatter (M). (N-O) Stage 10 embryos which are maternally deprived of indicated genes. Compared to control (N), simultaneous maternal depletion of *sac1* and *wun* result in worsening of PGC migration defects and leads to more precocious clumping of PGCs (O). (P) Quantification of comparison of PGC migration defects (n=15, 3 replicates) and significance calculated using Ordinary one-way ANOVA and Tukey's multiple comparison test \*\*\*\*p<0.0001, \*\*\*p<0.01. Diagonal lines represent the percentage of embryos that have PGCs that have not individualised by stage10. The gut outline is marked. The gonads at stage 13-14 are marked within dashed circles.

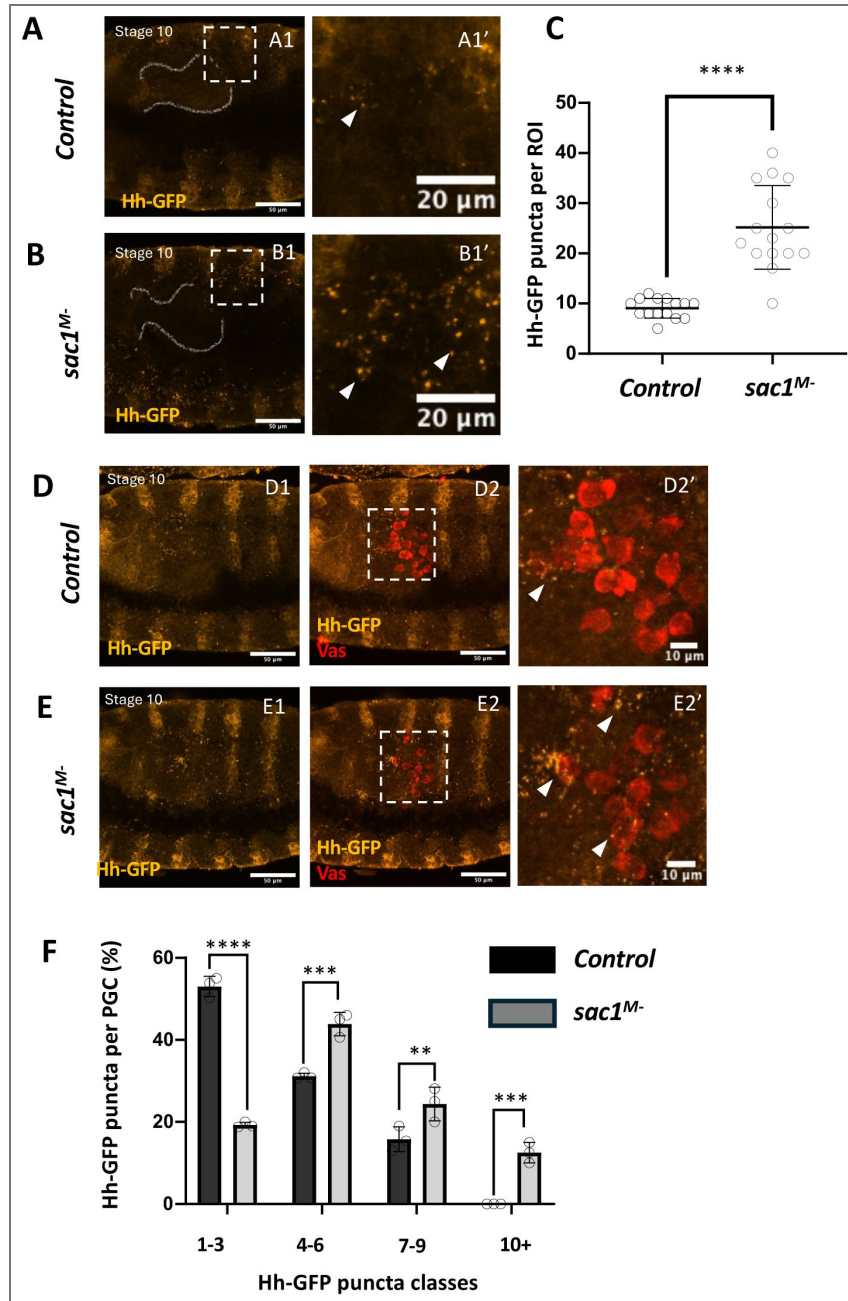


**Figure 7. Endogenous Hh-GFP specific puncta in the mesoderm and the adjacent PGCs are enhanced in *sac1<sup>M-</sup>* embryos.**

(A-B) Either *UAS-lexA RNAi* (control) or *UAS-sac1 RNAi* males were mated with *nos-Gal4* females. Virgin females carrying both the transgenes were subsequently mated with males expressing endogenous *hh-GFP*. Embryos resulting from this cross are maternally depleted of indicated genes, express endogenous *Hh-GFP* and are referred to as *lexA<sup>M-</sup>* or *sac1<sup>M-</sup>*. Compared to control (A) *sac1<sup>M-</sup>* embryos show higher number of *Hh-GFP* puncta (yellow) in the mesoderm (B). (C) The increase in *Hh-GFP* is quantified using an unpaired T-test. Individual *Hh-GFP* puncta were counted in 15 ROIs above gut, marked, per genotype. \*\*\*\* $p < 0.0001$ . (A1-B1) Embryos stained with anti-GFP (Yellow). Magnified insets are shown in (A1'-B1'). (D-E) Stage 10 embryos maternally depleted of the indicated gene, expressing endogenous *Hh-GFP*. Compared to control *lexA<sup>M-</sup>* (D), *sac1<sup>M-</sup>* embryos show higher number of *Hh-GFP* puncta in their PGCs. *Hh-GFP* stained with anti-GFP antibody (D1-E1, yellow) along with PGCS stained with anti-Vas (D2-E2, red). (F) Total number of puncta were counted in 12 PGCS per genotype across three replicates. The percentages of PGCS with 1-3, 4-6, 7-9 and 10+ *Hh-GFP* puncta are indicated in the graph and significance calculated using Two-way ANOVA and Dunnett's multiple comparison test. \*\*\*\* $p < 0.0001$ , \*\* $p < 0.01$ . (D2'-E2') are magnified insets. Arrowheads mark *Hh-GFP* puncta.

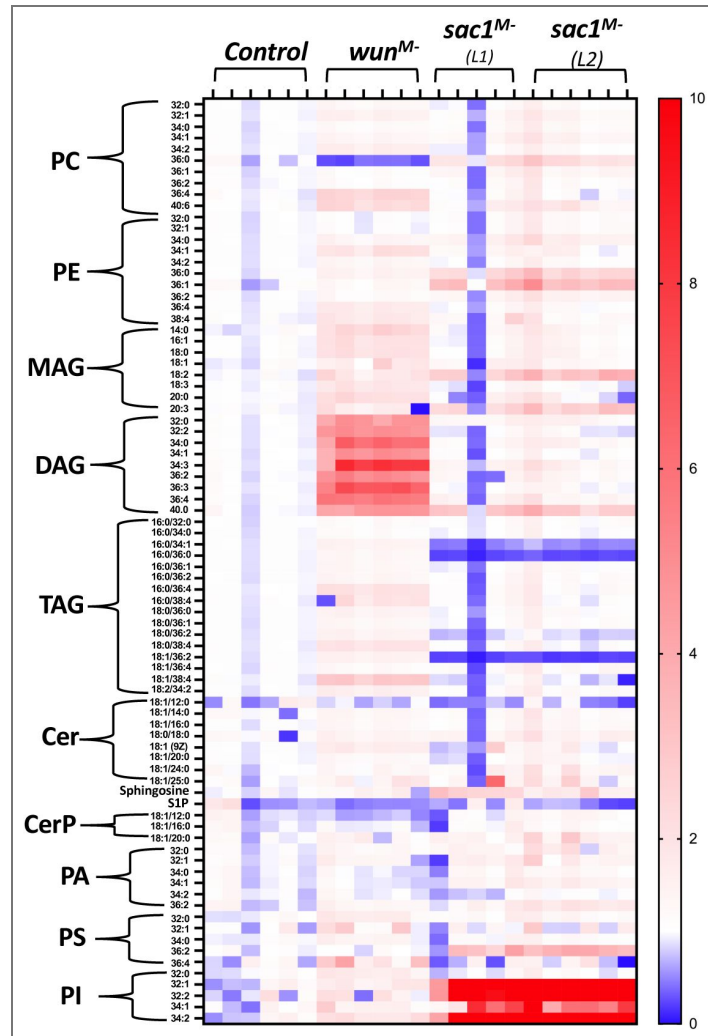


**Figure 8. Substrate specificity of Wun and Sac1.**

A heat map plot showing relative lipid levels in 4-8 hour old whole embryos, post-fertilisation after maternal depletion of *wun* and *sac1*. *lexA* knockdown embryos were used as controls. Lipidomic analysis shows that loss of *wun* leads to a specific increase in DAGs, whereas reducing *sac1* results in a considerable accumulation of PIs. Sac I is known to dephosphorylate Phospho-isomers of Phosphatidylinositols to generate PIs with a reduced number of phosphate residues. The Y-axis represents the lipid classes identified in the embryonic lysates, with individual rows corresponding to different attached fatty acids, listed by chain length and degree of (un)saturation. The X-axis represents the multiple replicate experiments for the genotypes represented.

Because compromising *sac1* has been reported to increase PI4P levels, we initially focused on phosphoinositide levels. Notably, embryos maternally compromised for *sac1* showed increased levels of various phosphoinositide species (estimated and collectively represented as PI) compared with control samples. Evidently, PI levels are not appreciably altered in *wun*<sup>M-</sup> embryos. Surprisingly, however, DAG levels are considerably elevated in *wun*<sup>M-</sup> extracts as compared to either the control or the *sac1*<sup>M-</sup> samples. Membrane-bound DAG subsequently participates in a variety of physiological alterations (Nilssen *et al.* 2005 [↗](#); Zhong *et al.* 2022 [↗](#); Falzone and Mackinnon 2023 [↗](#))

Since DAG is not phosphorylated, its accumulation in *wun*<sup>M-</sup> extracts cannot be attributed directly to the loss of *wun* activity. Instead, the accumulation of elevated levels of DAG must be an indirect consequence of the loss of *wun* function. Elevated levels of DAG are typically generated by the activation of phospholipase C, which breaks down PIP2 into DAG and IP3. Typically, signaling pathways that utilise GPCRs can turn on phospholipase C by promoting the dissociation of *Gα* from the *Gβγ* dimer. Phospholipase C can also be activated by excessive levels of lysophosphatidic acid (LPA) which is the only known *wun* substrate (Burnett and Howard 2003 [↗](#)). Thus, the specific and robust increase in DAG levels upon compromising *Wun* activity dovetails nicely with aberrant localization of *Smo*, a GPCR involved in mediating Hh signal. Together these data support the notion that *Wunen*, likely employs Hh and the downstream components of the signaling cascade to engineer germ cell repulsion.

## Discussion

Migrating cells in different developmental contexts are exposed to a plethora of signals in their cellular environment. Only a select few of these signals has the ability to guide motility of these cells and can function as either attractive or repulsive cues. Conversely, the migrating cells are also endowed with a restricted and well-calibrated ability to respond selectively to either move away from or towards the signal. For instance, axonal migration in vertebrate embryos is guided by attractive influence of Netrins and Sonic-hedgehog whereas they are repelled by BMP ligands (Tessier-Lavigne 1994 [↗](#); Butler and Dodd 2003 [↗](#); Charron *et al.* 2003 [↗](#); Wu *et al.* 2019 [↗](#)). PGC migration in *Drosophila* is engineered by *Hmgcr* and *Wun* dependent attractive and repulsive influences respectively. While Hh acts as an attractive ligand for migrating PGCs, no specific repulsive signal has been identified thus far. It has been proposed that components of the *Hmgcr* dependent enzymatic pathway harness attractive potential of SGP derived Hh signal. Data presented here document that repulsive influence mediated by *wun* also targets Hh, however, in a qualitatively opposite, antithetical manner. In the following, we will discuss how a competitive reciprocal balance between *hmgcr* and *wun* modulates Hh activity to carve the precise path of migrating PGCs.

The functioning of the *hh* signaling pathway in guiding the migration of the PGCs towards the SGPs is now reasonably well understood. Hh expressed by the SGPs is received by the migrating PGCs and its reception is transduced into their directed motility towards the source of the Hh. The response to the reception of the Hh ligand is highly polarized. Consequently, *Smo* is translocated from the cytoplasm to the membrane where it accumulates in a single sharp focus at the leading edge of the migrating PGCs. *Smo* subsequently recruits the GPCR *Tre1* to the membrane and *Tre1* activates F-actin assembly at the leading edge through the production of the signaling molecule PI(4,5)P<sub>2</sub> (Kim *et al.* 2021 [↗](#)).

To ensure that Hh ligands produced by the SGPs are preferentially received by the PGCs is especially critical to the deployment of *hh* as a guidance molecule in this context. Previous studies identified one such mechanism, namely the *potentiation of Hh transmission*. Though *hh* is widely expressed in ectodermal and mesodermal tissues throughout much of the embryo, its ability to attract migrating PGCs is primarily limited to the Hh produced by the SGPs (and their progenitors). One critical factor that distinguishes Hh produced by the SGPs from Hh expressed elsewhere in the embryo is *hmgcr*. *Hmgcr* and the downstream isoprenoid biosynthetic pathway function to greatly enhance the long-distance transmission of the Hh ligand. When *hmgcr* is expressed in other cell types or tissues, the endogenous Hh ligand expressed in these cells (or tissues) is able to compete

with the Hh ligand produced by the SGP and induce the mismigration of the PGCs. Thus, key to the potentiation activity of *hmgcr* is the fact its expression becomes progressively restricted to the SGPs during PGC migration. In addition to *hmgcr* several other genes important for the transmission are expressed in the mesoderm or posterior mesoderm (Ricardo and Lehmann 2009 [↗](#); Deshpande *et al.* 2013 [↗](#); Deshpande *et al.* 2016 [↗](#)). However, the potentiation of Hh transmission from the SGPs (and their mesodermal progenitors) by *hmgcr* is not in itself sufficient. We show here that the long-distance transmission of *hh* expressed in other cell types and tissues in the embryo must also be specifically suppressed in order to ensure that the migrating PGCs make their way to the SGPs. The suppression of *hh* signaling is mediated by the two Wun(s), Wun and Wun2. It was initially discovered that Wun functioned to repel migrating PGCs (Zhang *et al.* 1996 [↗](#); Zhang *et al.* 1997 [↗](#)). Subsequent studies identified the neighboring gene *wun2* (Starz-Gaiano *et al.* 2001 [↗](#); Hanyu-Nakamura *et al.* 2004 [↗](#)) and showed that it also functions to repel migrating PGCs. The two *wun*(s) encode lipid phosphate phosphatases and exhibit similar patterns of expression. Both gene products are maternally deposited and are present in the soma as well as the PGCs. In addition, both genes are zygotically expressed in the epidermis, gut primordium, and nervous system, tissues that migrating PGCs usually avoid.

While the repulsive activity of the *wun*(s) has been well documented, the mechanism of their action was not known. Using both the ‘loss’ and ‘gain-of-function’ experiments here we demonstrate that Wun(s) “repel” migrating PGCs because they are able to suppress the transmission of the Hh ligand—and this suppression of Hh transmission from other cell types and tissues enhances and refines the ability of Hh produced by the SGPs to attract the migrating PGCs. Perhaps the epistasis experiment presented in the manuscript constitutes the most direct demonstration of this mechanism of action involving antithetical activities of *Hmgcr* and Wun on Hh transmission. When *hmgcr* is ectopically expressed in the CNS, it induces PGC mismigration because it substantially enhances the transmission of the Hh ligand that is normally produced in the CNS. For this reason, the migration defects induced by ectopic *hmgcr* can be suppressed by co-expressing *hh-RNAi* with *hmgcr*. A similar suppression is observed for *wun*—in this case when *wun* is co-expressed with *hmgcr* using the same CNS driver.

Consistent with an ability to antagonize the *hh* signaling pathway, we find that when either *wun* or *wun2* is maternally depleted the *hh* signaling pathway is substantially upregulated. This enhanced activity is evident in the pattern of En expression in the embryonic ectoderm during mid-embryogenesis: there is an increase in the level of En expression and in the number of cells expressing En. Visualization of Hh produced by a BAC:*hh-GFP* rescue construct indicates that the transmission of Hh is upregulated when maternal *wun* is depleted. In a wild-type background Hh-GFP puncta decorate a subset of the migrating PGCs. In *wun<sup>M</sup>* embryos, the number of Hh-GFP puncta/PGCs increases. Excess Hh-GFP puncta are also seen in the mesoderm, indicating that there is a general enhancement in Hh transmission. The reception of the Hh ligand in migrating PGCs is also substantially altered. Instead of there being one primary membrane associated Smo focus, nearly half of the PGCs in *wun<sup>M</sup>* embryos have high levels of Smo all around their membranes or multiple Smo foci.

The enhanced transmission of the Hh ligand when *wun* is maternally depleted together with the *hmgcr/wun* epistasis experiments suggest that the Wun(s) function to mitigate the *hh* signaling pathway in *hh* expressing cells. On the other hand, the Wun(s) are known to be required not only in the soma but also in the PGCs themselves. In this case, the mislocalization of Smo in PGCs of *wun<sup>M</sup>* embryos could be due at least in part to an inappropriate cell autonomous activation of the *hh* signaling pathway in the receiving cells. As cytonemes extend from both Hh producing and Hh receiving cells in the imaginal discs, it is also conceivable that the loss of maternal *wun* in PGCs contributes to the increase in their labeling by Hh-GFP puncta. Two lines of evidence provide additional support for the idea that the *hh* pathway is upregulated in both the sending and receiving cells. The first would be the finding that *ptc*-like PGC migration defects are observed in both maternal *wun/wun2* RNAi knockdowns and in *wun/wun2* RNAi knockdowns in migrating PGCs. The second is the finding that a loss of another lipid phosphatase, *sac1*, also induces a similar spectrum of PGC migration defects. Consistently, as in the case of *wun*, embryos

compromised for *sac1* display PGC migration defects between stages 10-13 including retention of PGCs in the gut and reduction of PGC count in the coalesced gonads in a subset of embryos. Furthermore, as observed in *wun*<sup>M</sup>-embryos, *sac1*<sup>M</sup>-embryos also display an increased Hh association with migrating PGCs and an overall increase in the level of Hh in the surrounding mesoderm.

Analogous phenotypic consequences of the embryonic knockdowns of *wunen(s)* and *sac1* and their respective influence on Hh signaling on the embryonic PGCs are interesting in their own right. These observations coaxed us to revisit the reportedly crucial involvement of lipid metabolism and function vis-a-vis Hh signaling, PGC migration and their functional relationship. Wunen(s) have been characterized as lipid phosphate phosphatases (LPPs) based on their homology to the vertebrate LPPs. Substantial genetic characterization including rescue experiments has further supported the notion that LPP3 (human) and Wunen(s) likely share targets. By comparison, Sac1 has a relatively narrower and specific target range. Especially in the context of Hh signaling, it balances the Stt4 kinase activity to maintain the levels of PI4, which in turn, regulates membrane localization of Smo to modulate signaling downstream of Hh. Consequently, the phenotypic similarities between *wun* and *sac1*, in the context of PGC migration are intriguing.

Hence, we decided to assess whether they shared targets that may explain the similar phenotypes. The comparison of unbiased Lipidomics confirmed a few expectations but also threw up some unanticipated surprises. Foreseeably levels of different phosphoinositide species were substantially elevated upon the embryonic loss of *sac1*. Surprisingly however, a similar loss of *wun* did not alter PI or PA levels rendering them unlikely to be biologically relevant entities. Our current evidence supports the notion that Wunen(s) may function more broadly as a lipid metabolic or lipid-modifying enzyme(s), rather than lipid phosphatases per se. In this regard it is noteworthy that a specific and significant increase in DAG levels was observed upon loss of *wun*. The possible mechanistic underpinnings of this increase and its relationship with the phenotypic consequences are tantalizing as DAG accumulation is one of the indicators of activation of GPCR signalling (Nilssen *et al.* 2005 [↗](#); Zhong *et al.* 2022 [↗](#); Falzone and Mackinnon 2023 [↗](#)). Of note, Smo and Tre1, the two receptors demonstrated to act downstream of Hh signaling during PGC migration, are members of the GPCR family. Precocious clumping observed upon loss of Wun(s) could thus be an outcome of premature activation of one (or both) of these receptors.

*Drosophila* PGCs migrate in a calibrated manner across a complex cellular landscape. To arrive at their destination, germ cells ought to possess the ability to respond to the 'right' signal and ignore the 'wrong' ones. Moreover, PGCs must distinguish between the right signal emanating from the wrong source. Wunen(s) contribute to this ability as they constitute the other side of the coin. They hinder the ability of Hh to function as an attractive force if it is emanating from a 'wrong source'. The antithetical abilities of Hmgcr and Wun thus allow to fine tune the Hh signaling by potentiating the SGP derived 'right' signal and squelching the one emanating from the 'wrong' sources like ectoderm, nervous system etc. Moreover, this is unlikely to be an isolated instance and thus harbors tremendous potential as various disease conditions including metastasis involve long distance migration and inappropriate adhesion and lodging. Future experimental strategies will help elucidate mechanistic underpinnings of these events in the context of PGC migration and may also pave the way to understand its importance in other contexts where directed cell migration is a critical determinant of either normal or aberrant development.

## Materials & Methods

### Fly husbandry and stocks

Flies were raised on standard cornmeal agar at 25 °C unless stated otherwise. The *Drosophila melanogaster* lines, with IDs, used are: *CS* (BDSC\_64349), *UAS-lexA RNAi* (BDSC\_67947), *UAS-eGFP* (BDSC\_41552), *UAS-ptc RNAi* (BDSC\_55686), *UAS-smo RNAi V20* (BDSC\_53348), *UAS-smo RNAi V22* (BDSC\_43134), *nos-gal4 VP16* (BDSC\_4937), *UAS-sac1 RNAi* (BDSC\_56013), *UAS-sac1 RNAi* (VDRC #s

44376 and 37216), *maternal- $\alpha$ -tubulin-gal4-VP16* (*Mat-gal4* on both II and III, Gift from Daniel St. Johnston), *ptc-gal4 UAS-lacZ* (Gift from Matthew P Scott), *Hh:GFP Bac* (Gift from Thomas B. Kornberg), *UAS-wun-GFP* (Gift from Ken Howard),

For maternal knockdown experiments, we crossed *UAS-X RNAi* males, where 'X' is the gene to be knocked down, to maternal *gal4* driver females (either *mat-gal4 VP16* or *nos-gal4 VP16*). F2 embryos were collected for study, and since these are maternally compromised, their genotype is denoted as  $X^M$ . For zygotic knockdowns, denoted as  $X^Z$ , *UAS-X RNAi* males were crossed to maternal *gal4* drivers (*mat-gal4* or *nos-gal4*) females, and F1 embryos were used for study. *nos-gal4 VP16*, unlike *mat-gal4 VP16* is enriched specifically in PGCs. For zygotic overexpression of *wun*, we used F1 embryos (denoted as *wun*<sup>OE</sup>) derived from *mat-gal4* mothers crossed to males carrying the *UAS-wun-GFP* transgene.

## Embryo Fixation

Embryos were collected, typically aged 3-8 hours (with a focus on stages 10-11) or 0-12 hours (for overnight collections of later stages), in a sieve and dechorionated in 4% sodium hypochlorite for 90 seconds. After thorough washing with distilled water, the embryos were fixed in a 1:1 heptane:4% Paraformaldehyde (PFA) solution for 20 minutes, followed by removal of the PFA and a fresh heptane wash for 20 minutes. Furthermore, chilled methanol was added, and the embryos were devitellinized by vigorous shaking in a 1:1 heptane: methanol mixture. Devitellinized embryos settle at the bottom and are stored in 100% methanol at  $-20^{\circ}\text{C}$  until immunostaining.

## Immunostaining and Imaging

For immunostaining, embryos were rehydrated by four washes with 0.3% PBS-Triton X-100 (PBST), followed by blocking in 2% bovine serum albumin (BSA) in 0.3% PBS-T (blocking solution) for 1 hour at room temperature. Embryos were incubated overnight at  $4^{\circ}\text{C}$  with primary antibodies diluted in fresh blocking solution at the appropriate antibody-specific dilutions. The following primary antibodies in specified dilutions were used: Rabbit anti-Vasa (1:1000, Gift from Trudi Schüpbach), Mouse anti-En (1:50, DSHB), Mouse anti-Wg (1:20, DSHB), Chicken anti-GFP (1:500, Invitrogen), Mouse anti-Smo (1:50, DSHB), Mouse (1:20), and Chicken anti- $\beta$ gal (1:1000, Abcam). Following four washes with 0.3% PBS-T, the embryos were incubated in the appropriate secondary antibodies for 1 hour at room temperature. The following secondary antibodies were used in a 1:1000 dilution: goat anti-mouse AlexaFluor 488, goat anti-chicken AlexaFluor 568, goat anti-rabbit AlexaFluor 647 (1:1000, Invitrogen). Embryos were washed four times with 0.3% PBS-T, and Hoechst (1:1000 from a stock of 10 mg/ml) was added to the penultimate wash. All washes mentioned in the protocol are 10-15 mins each. Embryos were mounted in 20mM Tris pH=8, 0.5% n-propyl gallate, 90% glycerol and observed under a Nikon AX confocal microscope or an Evident inverted microscope (FV4000) using 40X and 20X objectives, respectively. Image processing was performed using the ImageJ program.

## Lipidomics

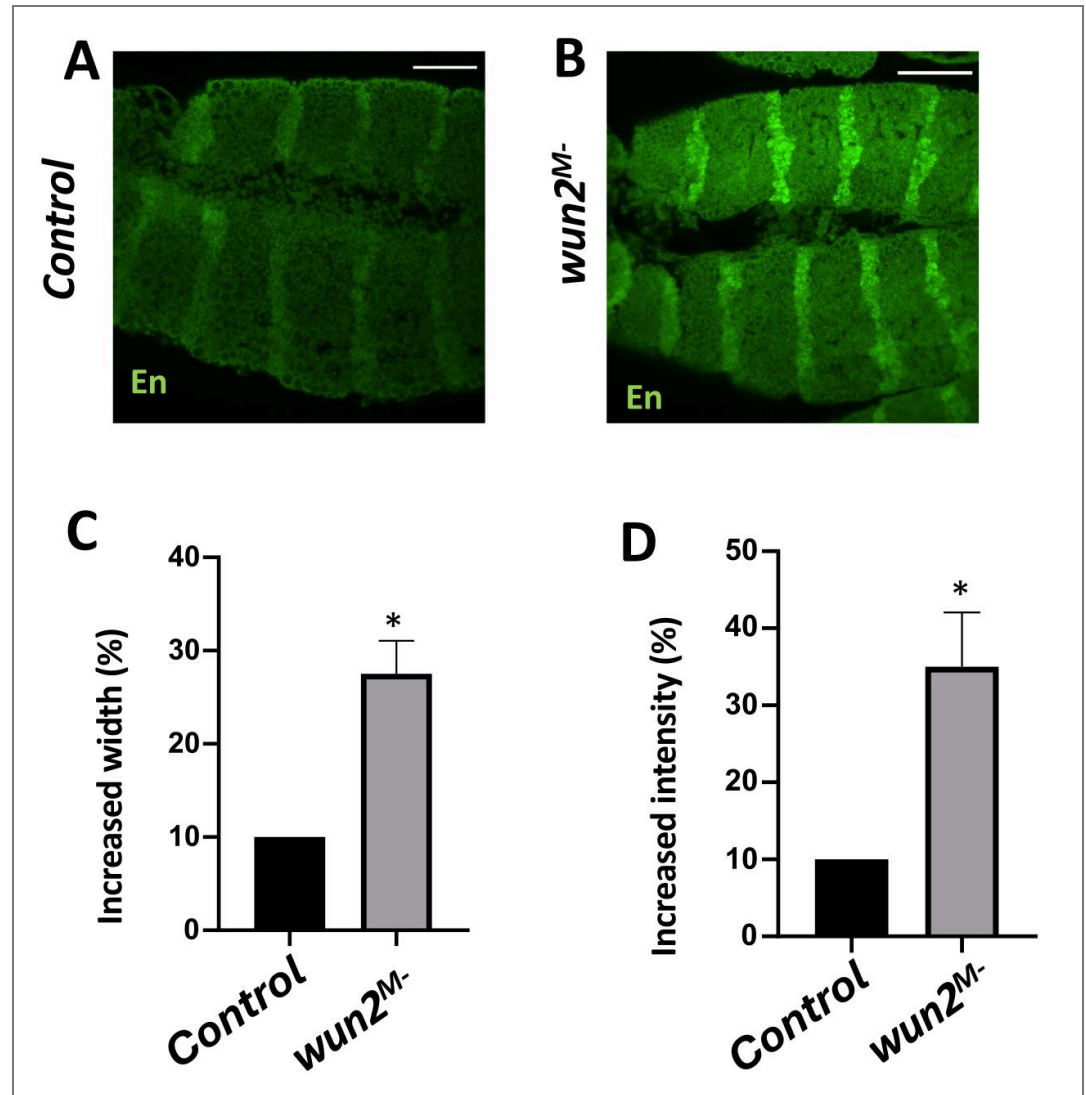
*Mat-Gal4* females were crossed with each of *UAS-mcherry RNAi*, *UAS-wun RNAi*, *UAS-Sac1 RNAi* (two lines L1 & L2). F2 embryos were collected for 0-4 hours and then aged at  $25^{\circ}\text{C}$  for 4 hours. Embryos were washed in 1x phosphate buffered saline (PBS) and snap frozen until further processing. For lipid extraction, the embryos were thawed on ice, suspended in 550  $\mu\text{L}$  of cold, sterile 1x PBS, pH 7.4 and homogenized using a tissue homogenizer (Bullet Blender24, Next Advance) with one scoop of glass beads (0.5-mm diameter; Next Advance) at a speed setting of 10 for 5 min at  $4^{\circ}\text{C}$ . The protein concentration of each lysate was estimated using the BCA protein assay kit (Pierce) according to the manufacturer's protocol. 500  $\mu\text{L}$  of the lysates were used for lipid extraction using established methods as described earlier (Kumar *et al.* 2024 [\[1\]](#)). Briefly, for each sample, 500  $\mu\text{L}$  lysate was transferred to a glass vial and vigorously mixed with 1.5 mL of 2:1 chloroform ( $\text{CHCl}_3$ ): methanol (MeOH) containing an internal standard mix [1 nmol each of pentadecanoic acid (Sigma-Aldrich, Catalog No. P6125, for negative ion mode analysis) and C17:0/20:4 phosphatidylcho line (Avanti Polar Lipids, Catalog No. LM-1002, for positive ion mode

analysis)]. The resulting mixture was centrifuged at 1500g for 15 min to separate the aqueous (top) and organic (bottom) layers, and the organic layer (bottom) was gently pipetted into a new glass vial. To enrich the extraction of phospholipids, the aqueous layer was acidified using 20  $\mu$ L formic acid (Merck, Catalog No. 5.33002) and further vigorously mixed with 1 mL of  $\text{CHCl}_3$ . The resulting mixture was again separated by centrifugation at 1500g for 15 min, and the organic layer (bottom) was separated and pooled with the organic extract from the previous extraction. The pooled organic phase was dried under a stream of nitrogen gas, resolubilized with 500  $\mu$ L of  $\text{CHCl}_3$ , and transferred to another glass vial to remove any trace aqueous contamination. The organic layer was dried again under a stream of nitrogen gas and resolubilized in 200  $\mu$ L of 2:1  $\text{CHCl}_3/\text{MeOH}$ , and 10  $\mu$ L of this was injected into an Agilent 6545 Quadrupole Time-of Flight (QTOF) LC-MS instrument for untargeted lipidomics measurements in each ion mode (positive and negative). A standard untargeted lipidomics run in positive or negative ion mode lasted 60 min, and the LC columns, solvents, and solvent gradients were identical to those previously reported by us (Kumar *et al.* 2024 [DOI](#)). All LC-MS/MS experiments were performed using an electrospray ionization (ESI) source with the following parameters: drying and sheath gas temperature = 320  $^{\circ}\text{C}$ ; drying and sheath gas flow rate = 10 L/min; fragmentor voltage = 150 V; capillary voltage = 4 kV; nebulizer pressure = 45 psi; and nozzle voltage = 1 kV. For the analysis of different lipids from the embryos, a Personal Compound Database Library (PCDL) curated for lipids was generated, and peaks corresponding to lipids were verified based on relative retention times, mass error threshold (20 ppm or less at MS1), and MS/MS fragments obtained. All lipid species were quantified by measuring the area under the curve relative to the respective internal standard and then normalizing this to the protein concentration of the respective sample.

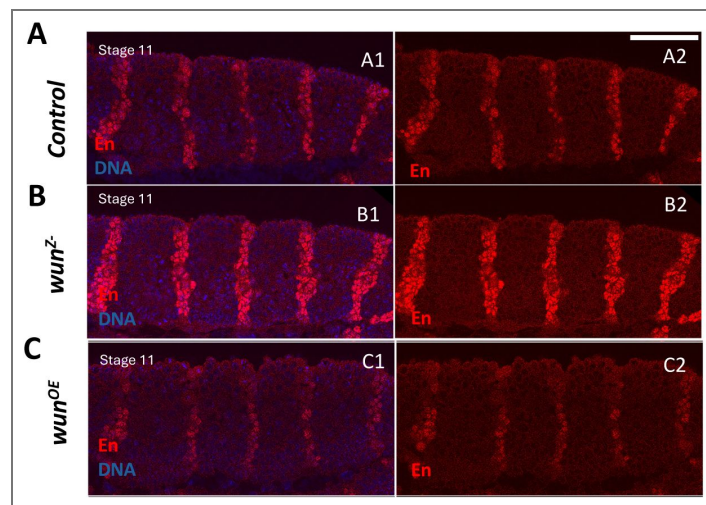
## Quantification & Statistical Analysis

The statistical analysis are detailed in figure legends. n in each graph represents the number of embryos, and N represents the number of replicates. To quantify PGC migration defects, embryos were stained with  $\alpha$ -Vasa antibody and imaged. In embryos older than stage 13, PGCs away from the somatic gonads were counted as mis-migrating cells. For maximum-intensity projections, equivalent slices were used across genotypes to ensure the best representation.

Figure supplements

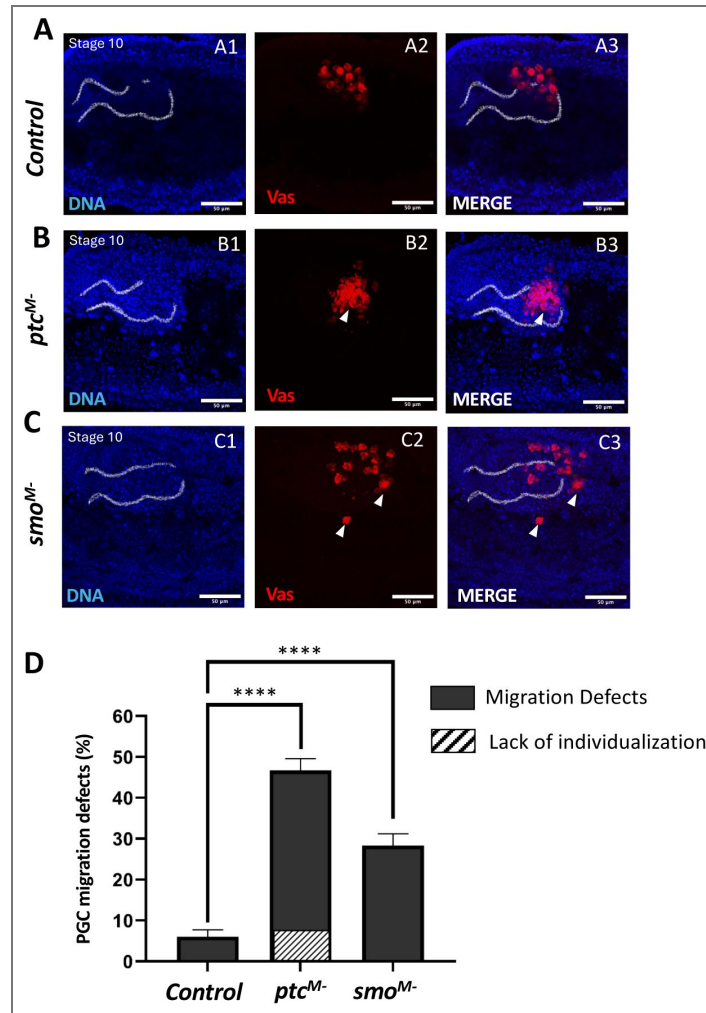


**Supplementary Figure 1.** Embryos maternally compromised for *wun2* display enhanced En expression in the ectoderm. (A-B) Stage 10 embryos maternally depleted of control *lexA* and *wun2*. Compared to the negative control *lex<sup>M-</sup>* embryos (A), a higher percentage of *wun2<sup>M-</sup>* embryos display as broader En stripes and increased levels of En protein (B). (C-D) Quantification of En stripe broadening (C) and increased En expression (D) in embryos. Significance was estimated using Ordinary one-way ANOVA (n=10 N=2), \*p<0.5.



**Supplementary Figure 2. Zygotic depletion or overexpression of *wun* affects En expression in the ectoderm.**

**(A-B)** Stage 11 embryos derived from *mat-gal4* mothers crossed to *UAS-RNAi* males of the indicated genotype. Compared to control *egfp<sup>2-</sup>* (A), *wun<sup>2-</sup>* embryos have increased En expression as well as broadening of En stripes (B). (C) On the contrary, zygotically overexpressing *wun* (*wun<sup>OE</sup>*) leads to decrease in En expression as well as thinning of the En stripe. All embryos were stained with anti-En antibodies and counter labeled with the DNA dye, Hoechst (A1-C1) Panels (A2-C2) display anti-En staining.

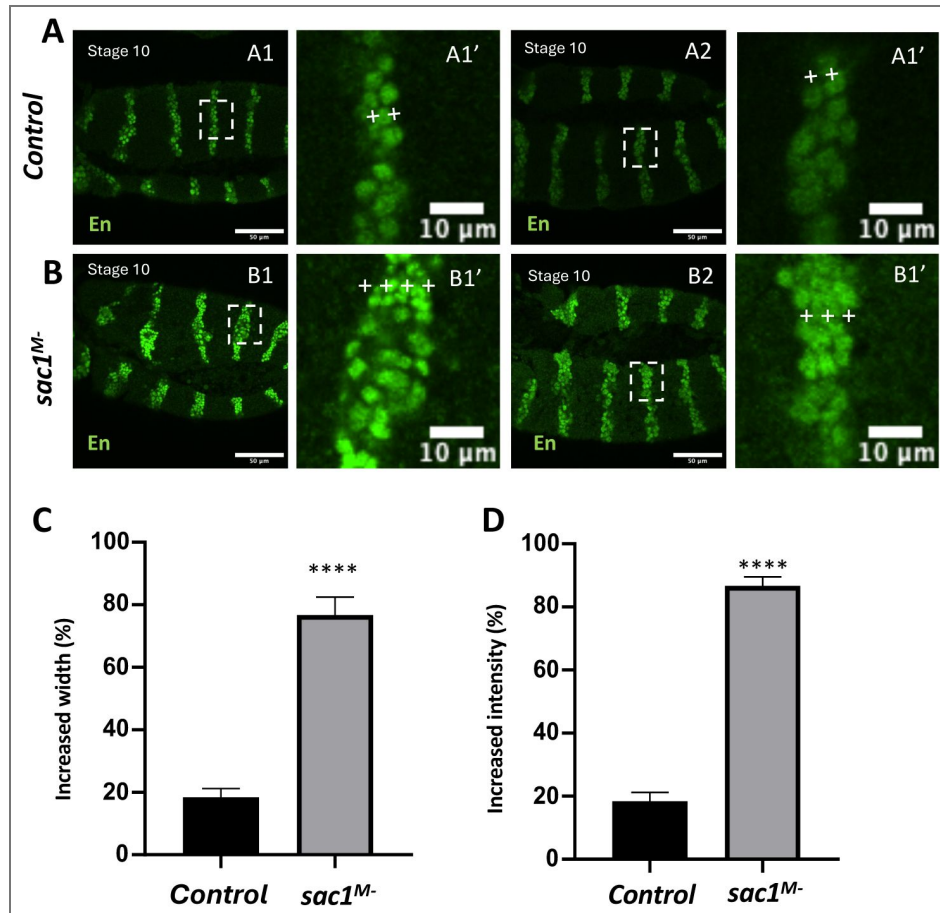


**Supplementary Figure 3. Maternal requirement of Hh receptors, *ptc*, and *smo* during PGC migration in early embryos.**

(A-C) Stage 10 embryos maternally deprived of indicated genes were laid by the nos-gal4>UAS-RNAi of indicated genes. PGCs in control *lexA<sup>M-</sup>* embryo display clearly individualized PGCs that traverse across the gut through its dorsal side (A). In contrast, PGCs in *ptc<sup>M-</sup>* embryos either clump and fail to individualize altogether (B) or show delayed migration through the gut possibly due to incomplete individualization. Conversely, PGCs of *smo<sup>M-</sup>* (C) are able to individualize like the control PGCs and exit the gut but start to scatter on their way to the mesoderm. Panels (A1-C1) display Hoechst staining, Panels (A3-C3) displayed merged images. Arrowheads mark mis-migrated embryos. Gut is outlined. (D) Aberrant migration of PGCs is quantified in graph using Ordinary one-way ANOVA and Tukey's multiple comparison test (n=12,3 replicates), \*\*\*\*p<0.0001. Diagonal lines represent percentage of embryos that have PGCs that have not individualized by stage10.

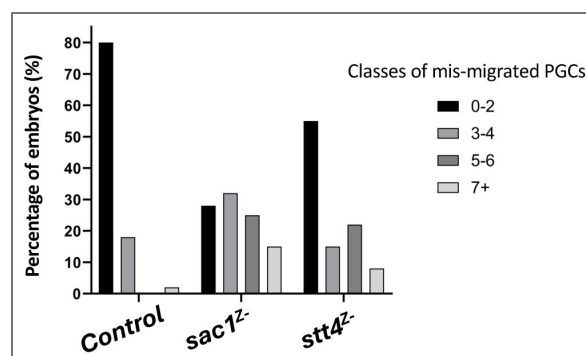
**Supplementary Figure 4. Embryos derived from mothers compromised for *sac1* (*sac1<sup>M-</sup>*) show elevated En expression in the ectoderm.**

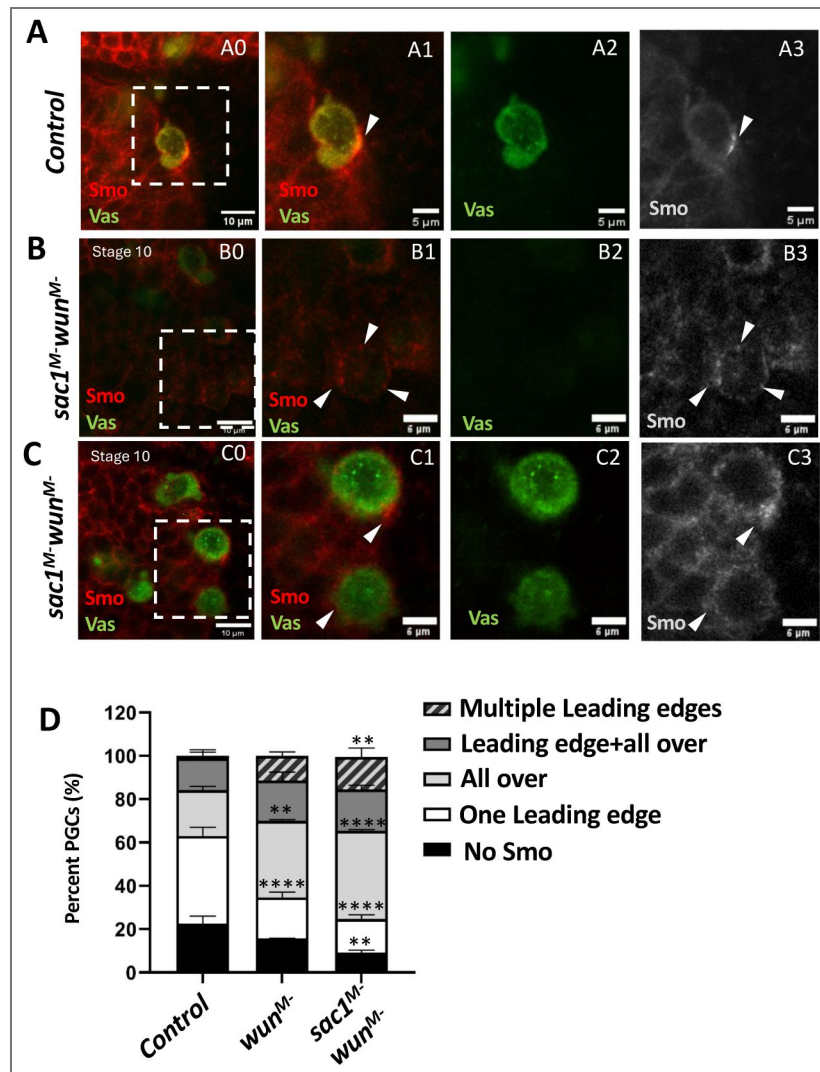
(A-B) Stage 10 Embryos derived from *nos-gal4>UAS-RNAi* were stained with anti-Engrailed (En) antibody (green) and DNA dye, Hoechst (not shown\*). Compared to the negative control *lex<sup>M-</sup>* (A1 and A2) embryos a significantly higher percentage of *sac1<sup>M-</sup>* (B1 and B2) embryos display expansion in the width of the individual stripes and increased level of En protein and. '+' mark is used for the cells positive for En in a stripe. Panels (A1',-A2' and B1'-B2') show magnified insets. (C-D) Quantification of En stripe broadening (C) and increased En expression (D) in embryos. Significance calculated using Ordinary one-way ANOVA (n=10 N=3), \*\*\*\*p<0.0001.



**Supplementary Figure 5. Zygotic depletion of lipid modification enzymes required for regulating Hh signalling results in germ cell migration defects.**

Bar graph showing the percentages of embryos of indicated genotypes with a given number of mis-migrating germ cells. Chi-square Goodness of Fit test was done for each genotype with the *Control* (n = 38), *sac1<sup>Z-</sup>* (n = 48) p = 2.01 x 10<sup>-54</sup>, *stt4<sup>Z-</sup>* (n = 32) p = 4.83 x 10<sup>-23</sup>.





**Supplementary Figure 6. Genetic interaction between *wun* and *sac1* enhances aberrant Smo localization.**

(A-C) Stage 10 embryos of the indicated genotype. In control *lexA<sup>M</sup>* embryos (A) Smo is localized at the leading edge (A0, magnified inset A1-A3). In contrast, in *sac1<sup>M-</sup>; wun<sup>M-</sup>* PGCs, multiple foci of Smo localisation are observed (B0, magnified inset B1-B3) or are present all over the PGC (C0, magnified inset C1-C3). All panels were equally edited with minimum intensity value at 10 and maximum intensity value at 100 using Fiji Image J. (D) Comparison of percentages of embryos of indicated genotypes having Smo localization as per mentioned classes were quantified (n=40-70 across replicates) using 2-way ANOVA and Tukey's multiple comparison test \*\*\* p<0.001 \*\* p<0.01.

## Data availability

All data generated or analyzed during this study are included in the manuscript and supporting files; source data files have been provided for all figures.

## Acknowledgements

We thank: Bloomington *Drosophila* Stock Centre (BDSC), supported by NIH grant P40OD018537, for fly stocks; Snehal Patil and Yashwant Pawar for fly media and stock maintenance; Microscopy facility at IISER Pune, managed by Dr Santosh Podder and Vijay Vitthal; Saddam Shekh for technical assistance and maintenance of the biological mass spectrometry facility at IISER Pune.

## Additional information

### Funding

GD's visits to IISER Pune (2023-2025) are supported by the Ministry of Education (MoE) Scheme for the promotion of Academic & Research Collaboration (SPARC), Grant ID SPARC-1587, managed by IIT Kharagpur, which facilitates collaboration between IISER Pune and Princeton University. Pratiksha Trust Extra-Mural Support for Transformational Aging Brain Research grant EMSTAR/2023/SL03 to GR, facilitated by the Centre for Brain Research (CBR), Indian Institute of Science, Bangalore. SSK acknowledges financial support from the Anusudhan National Research Foundation (ANRF), Government of India (Grants: Swarna Jayanti Fellowship SB/SJF/2021-22/01). SSK & GSR receive Intramural support from IISER Pune. The IISER *Drosophila* media and Stock Centre are supported by the National Facility for Gene Function in Health and Disease (NFGFHD) at IISER Pune, which in turn is supported by an infrastructure grant from the DBT, Govt. of India (BT/INF/22/SP17358/2016). AR is a graduate student supported by a research fellowship from the Department of Biotechnology (DBT), Govt. of India. AER is an undergraduate student supported by a KVPY/INSPIRE fellowship, Department of Science & Technology, Govt. of India.

### Contributions

GD conceptualized the project, with inputs from PS, SK and GSR. AR executed the experiments, with contributions from AER, JD, AI and GD. KK conducted the Lipidomics experiments under SK's supervision. GD wrote the initial draft, with input from AR, AER, KK, SSK, and GSR. All authors edited and refined the manuscript to its final form. GSR, GD, PS & SSK were responsible for funding acquisition, supervision and project management.

### Funding

Funder	Grant reference number	Author
Pratiksha Trust EMSTAR	EMSTAR/2023/5L.03	Girish S Ratnaparkhi
SPARC	1587	Girish Deshpande
Anusudhan National Research Foundation	SB/SJF/2021-22/01	Siddhesh S Kamat

### Author ORCID iDs

**Paul Schedl:**  <https://orcid.org/0000-0001-5704-2349>

**Siddhesh S Kamat:**  <https://orcid.org/0000-0001-6132-7574>

**Girish S Ratnaparkhi:**  <https://orcid.org/0000-0001-7615-3140>

## References

- Araujo SJ** (2015) The Hedgehog Signalling Pathway in Cell Migration and Guidance: What We Have Learned from *Drosophila melanogaster*. *Cancers* **7**:2012-2022 <https://doi.org/10.3390/cancers7040873> | PubMed
- Barton LJ**, Roa-de la Cruz L, Lehmann R, Lin B (2024) The journey of a generation: advances and promises in the study of primordial germ cell migration. *Development* **151** <https://doi.org/10.1242/dev.201102> | PubMed
- Bialistok T**, Manry D, Smith P, Ng C, Kim Y, et al. (2019) Functional analysis of Niemann-Pick disease type C family protein, NPC1a, in *Drosophila melanogaster*. *Development* **146** <https://doi.org/10.1242/dev.168427> | PubMed
- Briscoe J**, Chen Y, Jessell TM, Struhl G (2001) A hedgehog-insensitive form of patched provides evidence for direct long-range morphogen activity of sonic hedgehog in the neural tube. *Mol Cell* **7**:1279-1291 [https://doi.org/10.1016/s1097-2765\(01\)00271-4](https://doi.org/10.1016/s1097-2765(01)00271-4) | PubMed
- Burnett C**, Howard K (2003) Fly and mammalian lipid phosphate phosphatase isoforms differ in activity both in vitro and in vivo. *EMBO Rep* **4**:793-799 <https://doi.org/10.1038/sj.embor.embor900> | PubMed
- Burnett C**, Makridou P, Hewlett L, Howard K (2004) Lipid phosphate phosphatases dimerise, but this interaction is not required for in vivo activity. *BMC Biochem* **5**:2 <https://doi.org/10.1186/1471-2091-5-2> | PubMed
- Butler SJ**, Dodd J (2003) A role for BMP heterodimers in roof plate-mediated repulsion of commissural axons. *Neuron* **38**:389-401 [https://doi.org/10.1016/s0896-6273\(03\)00254-x](https://doi.org/10.1016/s0896-6273(03)00254-x) | PubMed
- Campanale JP**, Montell DJ (2023) Who's really in charge: Diverse follower cell behaviors in collective cell migration. *Curr Opin Cell Biol* **81**:102160 <https://doi.org/10.1016/j.ceb.2023.102160> | PubMed
- Casali A**, Struhl G (2004) Reading the Hedgehog morphogen gradient by measuring the ratio of bound to unbound Patched protein. *Nature* **431**:76-80 <https://doi.org/10.1038/nature02835> | PubMed
- Charron F**, Stein E, Jeong J, McMahon AP, Tessier-Lavigne M (2003) The morphogen sonic hedgehog is an axonal chemoattractant that collaborates with netrin-1 in midline axon guidance. *Cell* **113**:11-23 [https://doi.org/10.1016/s0092-8674\(03\)00199-5](https://doi.org/10.1016/s0092-8674(03)00199-5) | PubMed
- Chen R**, Grill S, Lin B, Saiduddin M, Lehmann R (2025) Origin and establishment of the germline in *Drosophila melanogaster*. *Genetics* **229** <https://doi.org/10.1093/genetics/iyae217> | PubMed
- Chen W**, Huang H, Hatori R, Kornberg TB (2017) Essential basal cytonemes take up Hedgehog in the *Drosophila* wing imaginal disc. *Development* **144**:3134-3144 <https://doi.org/10.1242/dev.149856> | PubMed
- Chen Y**, Struhl G (1998) In vivo evidence that Patched and Smoothed constitute distinct binding and transducing components of a Hedgehog receptor complex. *Development* **125**:4943-4948 <https://doi.org/10.1242/dev.125.24.4943> | PubMed
- Chowdhury MAH**, Kandel R, Reinemann DN (2026) Dissecting Cytoskeletal Crosstalk Through Reconstituted Actin-Microtubule Systems. *Mol Biol Cell* mbcE25080396 <https://doi.org/10.1091/mbc.e25-08-0396> | PubMed
- Del Bel LM**, Griffiths N, Wilk R, Wei HC, Blagoveshchenskaya A, et al. (2018) The phosphoinositide phosphatase Sac1 regulates cell shape and microtubule stability in the developing *Drosophila* eye. *Development* **145** <https://doi.org/10.1242/dev.151571> | PubMed
- Deshpande G**, Godishala A, Schedl P (2009) Ggamma1, a downstream target for the hmgcr-isoprenoid biosynthetic pathway, is required for releasing the Hedgehog ligand and directing germ cell migration. *PLoS Genet* **5**:e1000333 <https://doi.org/10.1371/journal.pgen.1000333> | PubMed
- Deshpande G**, Kim JH, Hanlon CD, Schedl P, Andrew DJ (2025) Hedgehog and *Drosophila* germ cell migration. *Development* **152** <https://doi.org/10.1242/dev.205291> | PubMed

- Deshpande G**, Manry D, Jourjine N, Mogila V, Mozes H, et al. (2016) Role of the ABC transporter Mdr49 in Hedgehog signaling and germ cell migration. *Development* **143**:2111-2120 <https://doi.org/10.1242/dev.133587> | PubMed
- Deshpande G**, Ng C, Jourjine N, Chiew JW, Dasilva J, et al. (2023) Hedgehog signaling guides migration of primordial germ cells to the Drosophila somatic gonad. *Genetics* **225** <https://doi.org/10.1093/genetics/iyad165> | PubMed
- Deshpande G**, Schedl P (2005) HMGCoA reductase potentiates hedgehog signaling in Drosophila melanogaster. *Dev Cell* **9**:629-638 <https://doi.org/10.1016/j.devcel.2005.09.014> | PubMed
- Deshpande G**, Swanhart L, Chiang P, Schedl P (2001) Hedgehog signaling in germ cell migration. *Cell* **106**:759-769 [https://doi.org/10.1016/s0092-8674\(01\)00488-3](https://doi.org/10.1016/s0092-8674(01)00488-3) | PubMed
- Deshpande G**, Zhou K, Wan JY, Friedrich J, Jourjine N, et al. (2013) The hedgehog pathway gene shifted functions together with the hmgcr-dependent isoprenoid biosynthetic pathway to orchestrate germ cell migration. *PLoS Genet* **9**:e1003720 <https://doi.org/10.1371/journal.pgen.1003720> | PubMed
- Diaz J**, Patkunarajah A, Mayor R (2025) Cell migration during development: Is it always collective and never as a single cell?. *Curr Top Dev Biol* **164**:153-185 <https://doi.org/10.1016/bs.ctdb.2024.10.004> | PubMed
- Dillon DA**, Chen X, Zeimetz GM, Wu WI, Waggoner DW, et al. (1997) Mammalian Mg<sup>2+</sup>-independent phosphatidate phosphatase (PAP2) displays diacylglycerol pyrophosphate phosphatase activity. *J Biol Chem* **272**:10361-10366 <https://doi.org/10.1074/jbc.272.16.10361> | PubMed
- Falzone ME**, MacKinnon R (2023) The mechanism of Galpha(q) regulation of PLCbeta3-catalyzed PIP2 hydrolysis. *Proc Natl Acad Sci U S A* **120**:e2315011120 <https://doi.org/10.1073/pnas.2315011120> | PubMed
- Hanyu-Nakamura K**, Kobayashi S, Nakamura A (2004) Germ cell-autonomous Wunen2 is required for germline development in Drosophila embryos. *Development* **131**:4545-4553 <https://doi.org/10.1242/dev.01321> | PubMed
- Hu A**, Song BL (2019) The interplay of Patched, Smoothed and cholesterol in Hedgehog signaling. *Curr Opin Cell Biol* **61**:31-38 <https://doi.org/10.1016/j.ceb.2019.06.008> | PubMed
- Ingham PW** (2022) Hedgehog signaling. *Curr Top Dev Biol* **149**:1-58 <https://doi.org/10.1016/bs.ctdb.2022.04.003> | PubMed
- Jasinska R**, Zhang QX, Pilquil C, Singh I, Xu J, et al. (1999) Lipid phosphate phosphohydrolase-1 degrades exogenous glycerolipid and sphingolipid phosphate esters. *Biochem J* **340**:677-686 <https://doi.org/10.1042/bj3400677> | PubMed
- Johnson RL**, Milenkovic L, Scott MP (2000) In vivo functions of the patched protein: requirement of the C terminus for target gene inactivation but not Hedgehog sequestration. *Mol Cell* **6**:467-478 [https://doi.org/10.1016/s1097-2765\(00\)00045-9](https://doi.org/10.1016/s1097-2765(00)00045-9) | PubMed
- Kim JH**, Hanlon CD, Vohra S, Devreotes PN, Andrew DJ (2021) Hedgehog signaling and Tre1 regulate actin dynamics through PI(4,5)P(2) to direct migration of Drosophila embryonic germ cells. *Cell Rep* **34**:108799 <https://doi.org/10.1016/j.celrep.2021.108799> | PubMed
- Kumar K**, Pazare M, Ratnaparkhi GS, Kamat SS (2024) CG17192 is a Phospholipase That Regulates Signaling Lipids in the Drosophila Gut upon Infection. *Biochemistry* **63**:3000-3010 <https://doi.org/10.1021/acs.biochem.4c00579> | PubMed
- Kunwar PS**, Siekhaus DE, Lehmann R (2006) In vivo migration: a germ cell perspective. *Annu Rev Cell Dev Biol* **22**:237-265 <https://doi.org/10.1146/annurev.cellbio.22.010305.103337> | PubMed
- LeBlanc MG**, Lehmann R (2017) Domain-specific control of germ cell polarity and migration by multifunction Tre1 GPCR. *J Cell Biol* **216**:2945-2958 <https://doi.org/10.1083/jcb.201612053> | PubMed
- Nilssen LS**, Dajani O, Christoffersen T, Sandnes D (2005) Sustained diacylglycerol accumulation resulting from prolonged G protein-coupled receptor agonist-induced phosphoinositide breakdown in hepatocytes. *J Cell Biochem* **94**:389-402 <https://doi.org/10.1002/jcb.20260> | PubMed

- Paluch EK, Aspalter IM, Sixt M (2016) Focal Adhesion-Independent Cell Migration. *Annu Rev Cell Dev Biol* **32**:469-490 <https://doi.org/10.1146/annurev-cellbio-111315-125341> | PubMed
- Renault AD, Kunwar PS, Lehmann R (2010) Lipid phosphate phosphatase activity regulates dispersal and bilateral sorting of embryonic germ cells in *Drosophila*. *Development* **137**:1815-1823 <https://doi.org/10.1242/dev.046110> | PubMed
- Renault AD, Lehmann R (2006) Follow the fatty brick road: lipid signaling in cell migration. *Curr Opin Genet Dev* **16**:348-354 <https://doi.org/10.1016/j.gde.2006.06.015> | PubMed
- Renault AD, Sigal YJ, Morris AJ, Lehmann R (2004) Soma-germ line competition for lipid phosphate uptake regulates germ cell migration and survival. *Science* **305**:1963-1966 <https://doi.org/10.1126/science.1102421> | PubMed
- Ricardo S, Lehmann R (2009) An ABC transporter controls export of a *Drosophila* germ cell attractant. *Science* **323**:943-946 <https://doi.org/10.1126/science.1166239> | PubMed
- Roper K (2025) Supracellular actomyosin assemblies: master coordinators of development. *Development* **152** <https://doi.org/10.1242/dev.204896> | PubMed
- Santos AC, Lehmann R (2004a) Germ cell specification and migration in *Drosophila* and beyond. *Curr Biol* **14**:R578-589 <https://doi.org/10.1016/j.cub.2004.07.018> | PubMed
- Santos AC, Lehmann R (2004b) Isoprenoids control germ cell migration downstream of HMGCoA reductase. *Dev Cell* **6**:283-293 [https://doi.org/10.1016/s1534-5807\(04\)00023-1](https://doi.org/10.1016/s1534-5807(04)00023-1) | PubMed
- Schick J, Ermlich L, Kuhl L, Hoffmann D, Raz E (2025) Single-cell migration in development - Lessons from germ cells. *Curr Top Dev Biol* **164**:1-27 <https://doi.org/10.1016/bs.ctdb.2025.01.002> | PubMed
- Starz-Gaiano M, Cho NK, Forbes A, Lehmann R (2001) Spatially restricted activity of a *Drosophila* lipid phosphatase guides migrating germ cells. *Development* **128**:983-991 <https://doi.org/10.1242/dev.128.6.983> | PubMed
- Tessier-Lavigne M (1994) Axon guidance by diffusible repellants and attractants. *Curr Opin Genet Dev* **4**:596-601 [https://doi.org/10.1016/0959-437x\(94\)90078-h](https://doi.org/10.1016/0959-437x(94)90078-h) | PubMed
- Wu Z, Makihara S, Yam PT, Teo S, Renier N, et al. (2019) Long-Range Guidance of Spinal Commissural Axons by Netrin1 and Sonic Hedgehog from Midline Floor Plate Cells. *Neuron* **101**:635-647. <https://doi.org/10.1016/j.neuron.2018.12.025> | PubMed
- Yavari A, Nagaraj R, Owusu-Ansah E, Follick A, Ngo K, et al. (2010) Role of lipid metabolism in smoothed derepression in hedgehog signaling. *Dev Cell* **19**:54-65 <https://doi.org/10.1016/j.devcel.2010.06.007> | PubMed
- Zhang N, Zhang J, Cheng Y, Howard K (1996) Identification and genetic analysis of *wunen*, a gene guiding *Drosophila melanogaster* germ cell migration. *Genetics* **143**:1231-1241 <https://doi.org/10.1093/genetics/143.3.1231> | PubMed
- Zhang N, Zhang J, Purcell KJ, Cheng Y, Howard K (1997) The *Drosophila* protein *Wunen* repels migrating germ cells. *Nature* **385**:64-67 <https://doi.org/10.1038/385064a0> | PubMed
- Zhang Y, Beachy PA (2023) Cellular and molecular mechanisms of Hedgehog signalling. *Nat Rev Mol Cell Biol* **24**:668-687 <https://doi.org/10.1038/s41580-023-00591-1> | PubMed
- Zhong T, Zhang W, Guo H, Pan X, Chen X, et al. (2022) The regulatory and modulatory roles of TRP family channels in malignant tumors and relevant therapeutic strategies. *Acta Pharm Sin B* **12**:1761-1780 <https://doi.org/10.1016/j.apsb.2021.11.001> | PubMed

## Peer reviews

### Reviewer #1 (Public review):

This manuscript addresses how PGCs migrate towards SGP in the *Drosophila* embryo. It's been shown that Hh produced by SGP acts as an attractive cue, and that *Wunen(s)* act as

repulsive cues. In this work, the authors propose that Wun and Wun2 refine PGC guidance by attenuating Hedgehog signalling coming from other tissues.

Overall, the study is potentially interesting and could make an important contribution to the field. The data shown support the idea that Wun/Wun2 negatively regulate Hh signalling and produce PGC migration phenotypes associated with Hh. However, in my opinion, there are two major questions that should be addressed.

(1) Which is the mechanism by which Wun/Wun2 attenuates Hh signalling? The authors propose that Wun/Wun2 block Hh ligand transmission, but their data could also be explained by other possibilities, such as altered Hh production, uptake, retention or degradation, among others. The authors should either show the effect of Wun/Wun2 in Hh transmission mechanistically or attenuate their claim.

(2) How do Wun/Wun2 attenuate Hh signalling in PGCs? The authors propose that Wun/Wun2 function both in somatic tissues and in PGCs, but these two sites of action may have very different mechanistic implications. In the soma, Wun/Wun2 could affect Hh transmission, but a PGC-autonomous role cannot be explained simply by reduced Hh ligand transmission from producing cells; it would more likely involve ligand uptake, receptor trafficking, intracellular degradation or altered PGC responsiveness. This distinction should be central to the interpretation of the data.

<https://doi.org/10.7554/eLife.111629.1.sa2>

## Reviewer #2 (Public review):

Summary:

In this submission, Roy et al. examine the process of *Drosophila* PGC migration. Directed cell migration requires the concerted activities of chemoattractants and repellents to guide cells to the correct locale. In their submission, the authors describe a role for regulated Hedgehog (Hh) signaling to inform PGC migration. In prior work, the authors reported that Hmgcr potentiates Hh signaling, providing a permissive axis. A gap in the field, however, was the identification of the repulsive cues that guide PGCs out of the midgut and toward the future gonad. In the current work, the authors report that two wunen genes (wunen and wunen 2) inhibit Hh signaling, thereby repressing Hh activity. The model is that Hmgcr and wunen(s) balance the transmission of Hh signals to enable effective PGC migration.

Strengths:

A strength of this work is the comprehensive genetic analysis performed by the authors. The authors examine zygotic versus maternal contributions, autonomous versus non-autonomous requirements, and use a variety of RNAi and mutant allele combinations to examine genetic requirements and interactions. Another strength is that the data presented are generally clear and well quantified. Insets are provided to enhance visualization, and relevant data are quantified through replicated experiments.

Weaknesses:

Weaknesses of the work include a lack of biochemical data to validate some of the proposed interactions. Although the authors do report lipidomics data, little is done with these findings to validate or place the results in the context of a mechanistic model. Despite these issues, the conclusions stated are generally well supported by the results.

<https://doi.org/10.7554/eLife.111629.1.sa1>

## Author response:

### **eLife Assessment**

*In this valuable manuscript, the authors tackle a highly relevant question in biology: how cells integrate attractive and repulsive cues to achieve directed migration. They present solid data demonstrating that two wunen genes act as negative regulators of Hedgehog signalling, thereby enabling efficient primordial germ cell (PGC) migration in Drosophila embryos. Beyond its immediate scope, this work has broader implications, particularly for understanding key mechanisms underlying complex processes such as cancer metastasis, where the coordinated interpretation of guidance cues is critical.*

Thank you for the reviews and the overall assessment of our manuscript. It is our impression that both the reviewers and the senior editor find the study interesting and potentially of general relevance. The reviewers have made specific suggestions to improve the manuscript. They have also recommended ways to uncover the mechanistic basis to add to the broad appeal of the findings.

To begin with, we would like to point out that since the discovery of Wunen in 1996 by Ken Howard and colleagues, a number of genetic and molecular studies have attempted to identify and characterize the putative target(s) of the two lipid phosphate phosphatase(s). We and others have shown that Hh acts as a guidance signal for the migrating PGCs. Our data demonstrating the ability of Wunen(s) to attenuate Hh signaling constitutes an important step in elucidating the molecular underpinnings of the repulsive activity of Wun(s) during PGC migration.

Thus, we feel the need to share these findings with the scientific community at this juncture. In the following, we will summarize our response to the relevant points included in the individual public critiques of the reviewers without going into specific details.

### **Public Reviews:**

#### **Reviewer #1 (Public review):**

*This manuscript addresses how PGCs migrate towards SGP in the Drosophila embryo. It's been shown that Hh produced by SGP acts as an attractive cue, and that Wunen(s) act as repulsive cues. In this work, the authors propose that Wun and Wun2 refine PGC guidance by attenuating Hedgehog signalling coming from other tissues.*

*Overall, the study is potentially interesting and could make an important contribution to the field. The data shown support the idea that Wun/Wun2 negatively regulate Hh signalling and produce PGC migration phenotypes associated with Hh. However, in my opinion, there are two major questions that should be addressed.*

*(1) Which is the mechanism by which Wun/Wun2 attenuates Hh signalling? The authors propose that Wun/Wun2 block Hh ligand transmission, but their data could also be explained by other possibilities, such as altered Hh production, uptake, retention or degradation, among others. The authors should either show the effect of Wun/Wun2 in Hh transmission mechanistically or attenuate their claim.*

(2) How do *Wun/Wun2* attenuate Hh signalling in PGCs? The authors propose that *Wun/Wun2* function both in somatic tissues and in PGCs, but these two sites of action may have very different mechanistic implications. In the soma, *Wun/Wun2* could affect Hh transmission, but a PGC-autonomous role cannot be explained simply by reduced Hh ligand transmission from producing cells; it would more likely involve ligand uptake, receptor trafficking, intracellular degradation or altered PGC responsiveness. This distinction should be central to the interpretation of the data.

We thank the reviewer for recognizing the importance of the problem and we are sensitive to both the points of criticism regarding the mechanism(s) *Wun*(s) may employ to downregulate Hh signalling.

The reviewer correctly pointed out that we singled out Hh transmission as the putative target of *Wun*(s) which need not be the case. We agree with this assessment and would like to thank the reviewer for pointing us in the right direction(s). Indeed, *Wun*(s) could act at several different levels to regulate Hh signalling including “Hh production, uptake, retention or degradation”. We will modify the text to incorporate these possibilities in the appropriate sections of the manuscript.

The only reason for the emphasis on the ‘Hh transmission’ in the text was to contrast it with *Hmgcr* which acts in a qualitatively opposite manner. *Hmgcr* potentiates Hh signalling by altering the range/strength of the Hh ligand in the embryonic context. This was also confirmed in the wing discs and adult wings as *hmgcr* mutants could dominantly suppress the wing duplications and abnormalities induced by the ‘gain of function’ allele of *hh* (*hh<sup>MRT</sup>*). Upon compromising *hmgcr*, Hh ligand was shown to be sequestered in the Hh producing cells in the ectoderm. However, we have not carried out similar experiments to either rule in or rule out the different possibilities suggested by the reviewer. We will ensure that the claims made in the manuscript will appropriately reflect the scope of the analysis and the related arguments will be suitably modified.

The reviewer also makes a very critical point regarding cell autonomous v/s cell non autonomous activities of *Wun*(s). We have briefly mentioned the possible role of individual *Wun*(s) in the SGPs/mesoderm as well as within the PGCs. It has not escaped our notice that *Wun*(s) could regulate Hh internalization within the PGCs or its subcellular compartmentalization (within the ER, golgi or lysosomes). *Wun*(s) could also act at the level of Hh reception by changing the activity/localization of Hh receptors, either Smoothed or Patched and could influence the outcome of the signaling pathway in a multi-pronged manner.

We appreciate the thoughtful suggestions and as recommended, future analysis will focus on these aspects. In our view, data included in the present version of the manuscript are novel and sufficient to argue a functional relationship between *Wun*(s) and Hh signalling which is qualitatively antagonistic to *Hmgcr*.

**Reviewer #2 (Public review):**

*Summary:*

*In this submission, Roy et al. examine the process of Drosophila PGC migration. Directed cell migration requires the concerted activities of chemoattractants and repellents to guide cells to the correct locale. In their submission, the authors describe a role for regulated Hedgehog (Hh) signaling to inform PGC migration. In prior work, the authors reported that Hmgcr potentiates Hh signaling, providing a permissive axis. A gap in the field, however, was the identification of the repulsive cues that guide PGCs out of the midgut and toward the future gonad. In the current work, the authors report that two wunen genes (wunen and wunen 2) inhibit Hh signaling, thereby repressing Hh activity.*

*The model is that Hmgcr and wunen(s) balance the transmission of Hh signals to enable effective PGC migration.*

*Strengths:*

*A strength of this work is the comprehensive genetic analysis performed by the authors. The authors examine zygotic versus maternal contributions, autonomous versus non-autonomous requirements, and use a variety of RNAi and mutant allele combinations to examine genetic requirements and interactions. Another strength is that the data presented are generally clear and well quantified. Insets are provided to enhance visualization, and relevant data are quantified through replicated experiments.*

*Weaknesses:*

*Weaknesses of the work include a lack of biochemical data to validate some of the proposed interactions. Although the authors do report lipidomics data, little is done with these findings to validate or place the results in the context of a mechanistic model. Despite these issues, the conclusions stated are generally well supported by the results.*

We would like to thank the reviewer for their positive feedback and a succinct description of the findings reported in the manuscript.

We agree that the mechanistic basis of DAG accumulation was not explored in this manuscript. Prior work in the Ratnaparkhi and Kamat labs identified a Serine hydrolase that functions as a phospholipase C in biochemical assays (Kumar et al., 2024, Biochemistry 63:3000-3010). We have since conducted several genetic experiments, and preliminary data indicate that, in the embryonic context, mutations in the specific Phospholipase C display phenotypes analogous to *wun(s)*. We hope to present these data along with the comparative molecular and biochemical analysis in the near future.

<https://doi.org/10.7554/eLife.111629.1.sa0>